# $N^6$-methyladenosine modification of HIV-1 RNA evades RIG-I-mediated sensing to suppresses type-I interferon induction in monocytic cells

**Short title**: $m^6A$ modification of HIV-1 RNA evades cellular sensing

Shuliang Chen[1,#,¶], Sameer Kumar[2,¶], Nagaraja Tirumuru[1], Jennifer L. Welch[3], Lulu Hu[4], Chuan He[4,5], Jack T. Stapleton[2,3], and Li Wu[2,*]

[1] Center for Retrovirus Research, Department of Veterinary Biosciences, The Ohio State University, Columbus, Ohio, United States of America

[2] Department of Microbiology and Immunology, Carver College of Medicine, University of Iowa, Iowa City, Iowa, United States of America

[3] Division of Infectious Diseases, Department of Internal Medicine, Carver College of Medicine, University of Iowa, The Iowa City VA Healthcare System, Iowa City, Iowa, United States of America

[4] Department of Chemistry, Department of Biochemistry and Molecular Biology, Institute for Biophysical Dynamics, University of Chicago, Chicago, Illinois, United States of America

[5] Howard Hughes Medical Institute, University of Chicago, Chicago, Illinois, United States of America

[#] Present address: School of Basic Medical Sciences, Wuhan University, Wuhan, Hubei, China.

* Corresponding author: E-mail: li-wu@uiowa.edu (LW)

[¶] These authors contributed equally to this work.

## Abstract

*N*$^6$-methyladenosine (m$^6$A) is a prevalent RNA modification that plays a key role in regulating eukaryotic cellular mRNA functions. RNA m$^6$A modification is regulated by two groups of cellular proteins, writers and erasers that add or remove m$^6$A, respectively. HIV-1 RNA contains m$^6$A modifications that modulate viral infection and gene expression in cells. However, it remains unclear whether m$^6$A modifications of HIV-1 RNA modulate innate immune responses in cells or HIV-1-infected individuals. Here we show that m$^6$A modification of HIV-1 RNA suppresses the expression of antiviral cytokine type-I interferon (IFN-I) in human monocytic cells. Transfection of differentiated monocytic cells with HIV-1 RNA fragments containing a single m$^6$A-modification significantly reduced IFN-I mRNA expression relative to their unmodified RNA counterparts. We generated HIV-1 with altered RNA m$^6$A levels by manipulating the expression of the m$^6$A erasers or pharmacological inhibition of m$^6$A addition in virus-producing cells. RNA transfection and viral infection of differentiated monocytic cells demonstrated that HIV-1 RNA with decreased m$^6$A levels enhanced IFN-I expression, whereas HIV-1 RNA with increased m$^6$A modifications had opposite effects. Our mechanistic studies revealed that m$^6$A of HIV-1 RNA escaped the RIG-I-mediated RNA sensing and activation of the transcription factors IRF3 and IRF7 that drive IFN-I gene expression. Moreover, RNA of peripheral blood mononuclear cells from HIV-1 viremic patients showed increased m$^6$A levels that correlated with increased *IFN-I* mRNA expression compared to levels from HIV-1-suppressed patients on antiretroviral therapy. Together, our results suggest that RNA m$^6$A modifications regulate viral replication and antiviral innate immune responses in HIV-1-infected individuals.

## Author Summary

HIV-1 is known as a weak inducer of antiviral cytokines including IFN-I, but it is unclear how HIV-1 evades innate immunity. Different types of RNA modifications including $m^6A$ within the HIV-1 genome modulate viral replication; however, the role of $m^6A$ modifications of HIV-1 RNA in regulating innate immune responses remains elusive. In this study, we found that HIV-1 RNA modified with $m^6A$ suppresses the expression of IFN-I in differentiated monocytic cells by avoiding innate immune detection of viral RNA mediated by RIG-I, an RNA sensor in host cells. We also observed significantly increased RNA $m^6A$ modifications of peripheral blood mononuclear cells from HIV-1 viremic patients compared to virally suppressed patients on combined antiretroviral therapy, suggesting a functional link between $m^6A$ modifications and antiretroviral treatment. Investigating the functions of $m^6A$ modifications of HIV-1 RNA in regulating innate immune sensing and IFN-I induction in monocytic cells can help understand the mechanisms of HIV-1 persistence.


**Keywords:** HIV-1, $m^6A$ RNA modification, IFN-I, RIG-I, innate immune responses.

## Introduction

Transcriptional modification of RNA in cells plays a crucial role in its stability, transportation, processing and thus regulation of gene expression. There are more than 160 RNA modifications identified in eukaryotes [1]. Methylation at the $N^6$ position of adenosine ($m^6A$) is a post-transcriptional RNA modification in internal and untranslated regions (UTRs) of eukaryotic mRNAs, microRNAs, small nuclear RNAs and long noncoding RNAs, which is important for RNA localization, stability and protein translation [1-5]. This methylation is controlled by two

types of protein factors in cells, comprised of the writer complex [(methyltransferase-like 3 (METTL3) and METTL14] to incorporate methylation, and the erasers [fat mass and obesity associated protein (FTO) and α-ketoglutarate dependent dioxygenase AlkB homolog 5 (ALKBH5)] to remove $m^6A$ modification [6-9]. RNA $m^6A$ modification has been discovered in several RNA and DNA viruses over the past 40 years, although its effects on the viral lifecycle remain not fully understood [10-15]. Recent advancement of RNA sequencing based strategies expanded the identification and characterization of $m^6A$ to several clinically significant human pathogens [16], including HIV-1 [17-19]. Increasing evidence suggests that $m^6A$ modification plays a major role in regulation of viral replication and gene expression [16] and the immune system [20].

In the early stage of virus infections, sensing viral nucleic acids in infected cells is a critical step to induce innate immune responses that can lead to production of antiviral cytokines, including IFN-I (mainly IFN-α and IFN-β) [21]. Genomic RNA of HIV-1 and other viruses can be detected by cytosolic sensors, including retinoic acid-induced gene I (RIG-I) and melanoma differentiation-associated gene 5 (MDA5) [21]. Detection of viral RNA by these sensors triggers activation of several cellular kinases, which phosphorylate interferon regulatory factors 3 and 7 (IRF3 and IRF7) to induce IFN-I expression [22, 23]. HIV-1 is a weak inducer of host innate immune responses [24, 25], and it evades immune recognition by direct targeting of immune pathways, interacting with cellular proteins, or masking the viral genome from the cytosolic sensors [24, 26, 27]. HIV-1 RNA can be sensed by both RIG-I and MDA5, whereas it has evolved multiple strategies to escape innate immune surveillance [23, 28]. A recent study showed that 2′-*O*-methylation in HIV-1 RNA prevents MDA5-mediated sensing in myeloid

cells, and thereby reduces IFN-I induction [29]. However, the role of m$^6$A in regulating innate immune responses to HIV-1 RNA and the underlying mechanisms have not been defined.

Our previous *in vitro* studies showed that HIV-1 infection or HIV-1 envelope protein treatment of CD4$^+$ T cells significantly up-regulates m$^6$A levels of cellular RNA independently of viral replication [30]. However, it remains unclear whether m$^6$A levels and IFN-I expression in HIV-1-infected individuals can be altered by effective antiretroviral therapy (ART), which leads to undetectable viral load in the vast majority of treated HIV-1 patients [31]. To address these fundamental questions and to better understand the role of m$^6$A in HIV-1 infection *in vivo*, we measured the levels of m$^6$A and IFN-I expression in peripheral blood mononuclear cells (PBMCs) of healthy donors, HIV-1 viremic patients before ART, and HIV-1 patients on ART.

Here we show that m$^6$A modifications of HIV-1 RNA reduce viral RNA sensing and the induction of IFN-I in differentiated monocytic cells. We found that m$^6$A-defective HIV-1 RNA induced IFN-I expression through RIG-I-mediated pathway, suggesting that m$^6$A is an immune evasion strategy of HIV-1. In contrast to *in vitro* results, we also observed significantly increased levels of m$^6$A RNA modifications and IFN-I expression in PBMCs from HIV-1 viremic patients compared to patients on ART. These results implicate that RNA m$^6$A modifications can contribute to regulation of viral replication, innate immune responses, and ART in HIV-1-infected individuals.

## Results

### A single m$^6$A modification of HIV-1 RNA oligos inhibits IFN-I induction in U937 cells.

To examine the effect of m$^6$A modification of HIV-1 RNA on IFN-I induction, we designed two different RNA oligos corresponding to two fragments of HIV-1 genome each with or without a

single m$^6$A modification [32] for transfection experiments. We have reported that these two m$^6$A modifications in the 5′ untranslated regions (UTR) of HIV-1 genome are important for HIV-1 RNA binding to the m$^6$A reader proteins (YTH domain family proteins 1-3) *in vitro* and viral replication in cells [32]. The m$^6$A-modified RNA oligos 1 and 2 (both 42 mer) contained a single m$^6$A-modified adenosine in the conserved GG**A**CU motif of the HIV-1 (NL4-3 strain) genome [32]. The m$^6$A modification of the oligos was confirmed by immunoblotting with equal amounts of RNAs using m$^6$A-specific antibodies (Fig. 1A and 1D). To mimic cellular responses to viral RNA in non-dividing macrophages, we differentiated monocytic U937 cells with phorbol 12-myristate 13-acetate (PMA) before transfection with the RNA oligos. Compared to unmethylated control (Ctrl) RNA, m$^6$A-modified RNA oligo 1 induced 3- to 4-fold lower ($P < 0.005$) levels of *IFN-α* and *IFN-β* mRNA in transfected cells (Fig. 1B and 1C). Similar results were obtained with transfection of oligo 2, although the effects were less significant compared to oligo 1 (Fig. 1E and 1F). These results indicate that m$^6$A modification of the 5′ UTR of HIV-1 RNA fragments inhibits IFN-I induction in differentiated U937 cells.

**Inhibition of m$^6$A modifications of HIV-1 RNA by FTO increases IFN-I induction.**

The m$^6$A erasers (FTO and ALKBH5) orchestrate cellular mRNA functions by removing m$^6$A modifications on mRNA [2]. To investigate whether m$^6$A modifications of HIV-1 genomic RNA could suppress IFN-I induction in cells, purified RNA from HIV-1 virions was demethylated with recombinant FTO *in vitro*, resulting in a 10-fold decrease in m$^6$A level relative to control HIV-1 RNAs (Fig. 2A). Transfection of m$^6$A-reduced HIV-1 RNA into U937 cells induced 3-fold higher *IFN-α* and *IFN-β* expression ($P < 0.0005$) compared to control RNAs (Fig. 2B and

2C), suggesting that m$^6$A modification of HIV-1 genomic RNA suppresses IFN-I induction in myeloid cells.

To determine the effect of m$^6$A of HIV-1 RNA on IFN-I induction during viral infection, HIV-1 containing lower levels of m$^6$A in viral RNA was generated by overexpression of the eraser FTO in HIV-1-producing HEK293T cells. Compared to the vector control, FTO overexpression in HEK293T cells had no significant effect on the expression of HIV-1 Gag and capsid (CA, or p24) proteins (Fig. 2D). HIV-1 derived from FTO-overexpressed HEK293T cells (m$^6$A-lower HIV-1) showed 10-fold lower m$^6$A levels of viral RNA compared to viruses derived from control cells (Fig. 2E). When PMA-differentiated U937 cells were transfected with RNA of m$^6$A-lower HIV-1, a 2-fold increase ($P < 0.05$) of *IFN-α* and *IFN-β* expression was observed compared to control HIV-1 RNA (Fig. 2F and 2G). As a positive control, poly(I:C) induced approximately 190-fold increases of *IFN-α* and *IFN-β* expression in transfected U937 cells (Fig. 2F and 2G). Moreover, differentiated U937 cells infected with m$^6$A-lower HIV-1 expressed 2-fold higher ($P < 0.05$) *IFN-α* and *IFN-β* relative to control HIV-1 (Fig. 2H and 2I). Thus, HIV-1 containing reduced RNA m$^6$A modifications induces higher *IFN-I* expression in differentiated U937 cells.

**Inhibition of m$^6$A modifications of HIV-1 RNA by ALKBH5 increases IFN-I induction.** To confirm the results of FTO treatment and overexpression, we also examined the effect of another m$^6$A eraser ALKBH5 on HIV-1 RNA-mediated IFN-I induction in PMA-differentiated U937 cells. ALKBH5 overexpression in HIV-1-producing HEK293T cells had no significant effect on the expression of HIV-1 Gag and CA (Fig. 3A). The m$^6$A modification of HIV-1 RNA generated from ALKBH5-overexpressed HEK293T cells showed a 2-fold decrease compared to

HIV-1 RNA from control cells (Fig. 3B). *IFN-α* and *IFN-β* levels in U937 cells transfected with HIV-1 RNA from ALKBH5-overexpressed HEK293T cells were 1.8-fold higher ($P < 0.05$) compared to that from control cells (Fig. 3C and 3D). Furthermore, infection of U937 cells with HIV-1 from ALKBH5-overexpressed HEK293T cells induced 2-fold higher *IFN-α* and *IFN-β* expression ($P < 0.0005$) compared to HIV-1 from control HEK293T cells (Fig. 3E and 3F). Thus, inhibition of m$^6$A modifications of HIV-1 RNA by eraser overexpression in virus-producing cells increases *IFN-I* induction in differentiated U937 cells.

**Knockout (KO) of erasers increases m$^6$A levels in HIV-1 RNA and reduces IFN-I induction.**

To validate the results from eraser overexpression, we constructed FTO-KO and ALKBH5-KO HEK293T cell lines by the CRISPR-Cas9 method. Next, these cell lines were transfected to generate HIV-1 with increased m$^6$A of viral RNA. Western blotting results showed that FTO and ALKBH5 were completely silenced and HIV-1 Gag protein expression was not significantly affected by FTO and ALKBH5 knockout (Fig. 4A). HIV-1 RNA from FTO-KO and ALKBH5-KO cells showed 7- and 25-fold higher m$^6$A levels, respectively, relative to that from control (Con-KO) cells (Fig. 4B). Transfection of PMA-differentiated U937 cells with HIV-1 RNA derived from FTO-KO or ALKBH5-KO cells showed a 3-4-fold decrease ($P < 0.05$) in *IFN-I* expression compared to that from Con-KO cells (Fig. 4C and 4D). Moreover, infection of PMA-differentiated U937 cells with HIV-1 from FTO-KO or ALKBH5-KO cells induced approximately 2-fold less *IFN-I* expression ($P <0.005$) compared to Con-KO cells (Fig. 4E and 4F). Thus, increasing m$^6$A levels in HIV-1 RNA by eraser KO in virus-producing cells reduces *IFN-I* induction in differentiated monocytic cells.

**m$^6$A-defective HIV-1 RNA induces IFN-I expression through IRF3 and IRF7 phosphorylation.**

We next investigated pharmacological inhibition of m$^6$A modification using 3-deazaadenosine (DAA), an inhibitor of S-Adenosylhomocysteine (SAH) hydrolase that can catalyze the reversible hydrolysis of SAH to adenosine and homocysteine [33]. DAA causes SAH accumulation thereby elevating the ratio of SAH to S-adenosylmethionine (SAM), a substrate of m$^6$A modification, and subsequent inhibition of SAM-dependent methyltransferases [33]. DAA-treatment of HEK293T cells did not affect HIV-1 production and release, but reduced m$^6$A level in HIV-1 RNA 7-fold compared to control cells (Fig. 5A and 5B). Transfection of PMA-differentiated U937 cells with purified RNA from HIV-1 produced from DAA-treated HEK293T cells (DAA-HIV-1) induced 15-fold and 2.3-fold higher *IFN-α* and *IFN-β* expression ($P <$ 0.0005), respectively (Fig. 5C and 5D). Moreover, infection of PMA-differentiated U937 cells with DAA- HIV-1 induced a 2-3-fold increase in *IFN-I* expression ($P < 0.0005$) compared to viruses from control HEK293T cells (Fig. 5E and 5F). These data further validate that m$^6$A of HIV-1 RNA suppresses IFN-I induction in differentiated monocytic cells.

Because IFN-I expression is predominately driven by IRF3 and IRF7 after their activation by phosphorylation upon virus infections [21, 34], we tested whether DAA-HIV affected phosphorylation of IRF3 and IRF7. Compared to mock-infected U937 cells, control HIV-1 and DAA-HIV-1 induced strong phosphorylation of IRF3 and IRF7 in differentiated U937 cells at 4 h post-infection (Fig. 5G). Notably, phosphorylation of IRF3 and IRF7 was 1.7-fold and 1.2-fold higher in U937 cells infected with DAA-HIV-1 relative to control HIV-1, respectively (Fig. 5G). These results suggest that inhibition of HIV-1 RNA m$^6$A modification

205 triggers innate immune responses by inducing IRF3/7-mediated IFN-I expression in myeloid
206 cells.
207
208 **RIG-I, but not MDA5, contributes to m$^6$A modification of HIV-1 RNA induced IFN-I**
209 **expression.**
210 To characterize the cellular sensing mechanisms of m$^6$A-defective HIV-1 RNA, RIG-I and
211 MDA5 in U937 cells were silenced by KO and shRNA, respectively. RIG-I-KO U937 cells were
212 constructed and undetectable RIG-I expression was confirmed (Fig. 6A). To test whether these
213 cells responded to RNA stimulation, poly(I:C) was transfected into cells and *IFN-I* expression
214 was measured. Compared to untransfected cells (mock), poly(I:C) transfection induced high
215 levels of *IFN-I* expression in RIG-I-KO and control U937 cells (Fig. 6B). As expected, the
216 induction of *IFN-I* by poly(I:C) was significantly reduced by 2-fold in RIG-I-KO U937 cells ($P$
217 $< 0.005$) compared to control cells (Fig. 6B), confirming that RIG-I acted as an RNA sensor to
218 induce *IFN-I* expression in these cells. In control U937 cells, transfection of single m$^6$A-
219 modified HIV-1 RNA oligos induced lower *IFN-I* expression ($P < 0.0001$) compared to
220 unmethylated RNA oligo counterparts (Fig. 6C and 6D). However, in RIG-I-silenced U937 cells,
221 transfection of m$^6$A-modified HIV-1 RNA oligos had no effect on *IFN-I* expression relative to
222 unmethylated control oligos (Fig. 6C and 6D), suggesting a pivotal role of RIG-I in sensing
223 m$^6$A-defective HIV-1 RNA.
224 Furthermore, we examined the potential role of MDA5 in sensing m$^6$A-defective HIV-1
225 RNA in monocytic cells. MDA5 expression was substantially reduced in differentiated U937
226 cells with MDA5 knockdown (shMDA5) compared to vector control (shCon) cells (Fig. 7A). As
227 a positive control, poly(I:C) transfection induced high levels of *IFN-I* expression in both shCon

and shMDA5 U937 cells. As expected, poly(I:C) transfection into shMDA5 U937 cells significantly decreased *IFN-I* levels relative to shCon cells (Fig. 7B). These cells were then examined for their ability to induce *IFN-I* expression by HIV-1 5′ UTR RNA oligos with or without single m$^6$A modification [32]. Compared to unmethylated HIV-1 RNA oligos, transfection of m$^6$A-modified HIV-1 RNA oligos reduced *IFN-I* expression in both shCon and shMDA5 U937 cells (Fig. 7C and 7D), suggesting that MDA5 is not a specific cellular sensor to detect m$^6$A-defective HIV-1 RNA in differentiated monocytic cells.

**HIV-1 infected patients have higher level of m$^6$A modification in the RNA of PBMCs.**

To explore the significance of m$^6$A modifications in HIV-1-infected individuals and investigate the effect of ART on m$^6$A levels, we measured the levels of m$^6$A and *IFN-I* mRNA in immune cells from HIV-1 viremic patients in comparison with healthy control donors and HIV-1 patients on ART. We obtained PBMCs from healthy control donors (n=9), HIV-1 viremic patients (n=6) with different viral load pre-therapy, and HIV-1-infected individuals on ART (n=16) whose viral load was undetectable for a minimum of 6 months (<20 copies/mL) (supplemental Table S1). The average m$^6$A level in total RNA of PBMCs from HIV-1 viremic patients was significantly higher ($P < 0.005$) compared to that from patients on ART (Fig. 8A and Supplemental Fig. S1A), suggesting an inverse correlation between viral load and m$^6$A level of patient PBMCs. A visible, but not statistically significant increase ($P = 0.27$) in cellular RNA m$^6$A level was observed in viremic patients compared to healthy individuals (Fig. 8A and Fig. S1A). This observation is also consistent with our previous results showing that HIV-1 infection or treatment of cells with HIV-1 envelope proteins (Env) upregulated m$^6$A levels in primary CD4$^+$ T-cells *in vitro* [30]. It

is possible that Env shedding from HIV-1 viremic patients could upregulate m$^6$A levels in PBMCs.

Next, the levels of *IFN-I* mRNA in PMBCs were measured to analyze potential correlations with the RNA m$^6$A levels. Compared to PBMCs from healthy donors, there was a trend of increase in *IFN-α* expression, and a significant increase in *IFN-β* expression in PBMCs from the viremic patients (Fig. 8B and 8C). Compared to PBMCs from the viremic patients, a significant decrease in both *IFN-α* and *IFN-β* expression ($P < 0.005$) was observed in patients on ART (Fig. 7B and 7C), suggesting that HIV-1 suppression by ART reduces innate immune responses to viral infection. Consistent with our results, a previous study [35] also reported similar results of decreased IFN-α expression in HIV-1 patients on ART compared to patients without ART.

Enhanced m$^6$A levels in viremic patients could not be attributed to inherent differences in the levels of m$^6$A writers and erasers, because there was no significant change in the expression of METTL3, FTO and ALKBH5 in PBMCs from the three groups (Fig. 8D and Fig. S1B). However, a slight increased level of METTL14 expression was observed in PBMCs from patients with ART compared to viremic patients (Fig. 8D and Fig. S1B). Together, these results suggest that HIV-1 infection upregulates the m$^6$A level of cellular RNA in PBMCs from viremic patients without altering the expression of the writers and erasers.

## Discussion

HIV-1 genomic RNA contains 10-14 sites of m$^6$A modifications in the 5′-, 3′-UTR and several coding regions [17-19]. Recent studies indicate that m$^6$A modification has important effects on HIV-1 replication, gene expression, and host responses to viral infection [30, 32, 36].

It has been shown that cellular enzymes involved in RNA m$^6$A modifications negatively regulate the innate immune response to infection of human cytomegalovirus, influenza A virus, adenovirus, or vesicular stomatitis virus by targeting the IFN-I pathway [37, 38]. A recent study showed that m$^6$A modifications of human metapneumovirus RNA mimic the host RNA to avoid RIG-I-mediated innate immune sensing, and thereby reduce the production of IFN-I and enhance viral replication [39]. However, it remains unknown whether m$^6$A modifications of HIV-1 RNA have any impact on innate immune responses.

In this study, we show that m$^6$A modifications of HIV-1 RNA act as a negative regulator of IFN-I induction by avoiding RIG-I-mediated RNA sensing in PMA-differentiated U937 cells. We observed that two different HIV-1 RNA oligos of the HIV-1 5′-UTR containing a single m$^6$A-modification significantly reduced IFN-I induction relative to their unmodified RNA counterparts. The different inhibitory effects on IFN-I induction by two m$^6$A-modified RNA oligos compared to their unmodified counterparts might be due to different sequences or conformation of the RNA fragments [32]. We also demonstrated that HIV-1 RNA with decreased m$^6$A levels enhanced IFN-I expression, but HIV-1 RNA with increased m$^6$A modifications had opposite effects. Our results suggest that HIV-1 genomic RNA and viral transcripts are masked by m$^6$A modifications to avoid RIG-I-mediated sensing and IFN-I induction during viral infection. Thus, HIV-1 has likely evolved an immune evasion strategy through m$^6$A modification of viral RNA (Fig. S2).

Several RNA modifications, such as N-1-methylpseudouridine, 5-methylcytidine (m$^5$C), 5-hydroxymethylcytidine, 5-methoxycytidine, and 2′ fluoro-deoxyribose, have significant impact on RIG-I- and MDA5-mediated RNA sensing [40]. In addition to m$^6$A modification, HIV-1 genomic RNA contains eight types of epitranscriptomic modifications that are higher than the

296 average cellular mRNA, with $m^5C$ and 2′-*O*-methyl modifications being most prevalent [41]. It is
297 possible that HIV-1 RNA exploits multiple epitranscriptomic modifications to avoid innate
298 sensing as mechanisms of immune evasion. This possibility may explain how HIV-1 is able to
299 avoid innate immune responses to establish persistent and latent infection even in patients on
300 combined ART [31].

301 The IFN-I gene itself is $m^6A$-modified and targets its destabilization for the maintenance
302 of homeostatic state in mouse and humans [38]. Rubio *et al.* showed that, following human
303 cytomegalovirus infection, depletion of METTL14 or increase in ALKBH5 proteins leads to
304 decrease level of $m^6A$ in IFN-β gene and stabilizes and elevates the IFN-I response [37]. In this
305 study, we observed increased $m^6A$ levels in cellular RNA of PBMCs from HIV-1 viremic
306 patients compared to HIV-1 suppressed patients on ART. However, we did not observe
307 significant changes in the levels of $m^6A$ writers and erasers in PMBCs from healthy donor, HIV-
308 1 viremic patients, and HIV-1 patients on ART. These results are consistent with our previous
309 data showing increased $m^6A$ levels in HIV-1 infected primary $CD4^+$ T-cells in the absence of
310 altered expression of $m^6A$ writers or erasers [30]. It is possible that HIV-1 may modulate the
311 activity or localization of writers or eraser, thereby upregulating $m^6A$ levels in HIV-1 infected
312 cells. It remains to be established whether $m^6A$ modification of HIV-1 RNA regulate innate
313 immune responses in primary $CD4^+$ T-cells or macrophages.

314 We found that $m^6A$-modified HIV-1 reduces the activation of IRF3 and IRF7 through
315 RIG-I-mediated signaling to suppress IFN-I induction. However, it remains unclear how $m^6A$
316 modifications of HIV-1 RNA reduces phosphorylation of IRF3 and IRF7 during early stage of
317 HIV-1 infection. Previous studies suggest that HIV-1 proteins can target several cellular RNA
318 and DNA sensors including RIG-I to surpass the IFN-I response [42-45]. Moreover, HIV-1 can

also target downstream proteins in the IFN-I pathway including IRF3 and IRF7 to contribute to chronic and persistent infection [46-50]. For example, HIV-1 Vpr protein mediates degradation of IRF3 to avoid the innate antiviral immune response [51].

Durbin *et al.* showed that a RIG-I-activating RNA ligand, the 106-nucleotide polyU/UC sequence derived from the 3′ UTR of hepatitis C virus with $m^6A$ modification bound RIG-I with low affinity and did not trigger the conversion to the activated RIG-I conformer and thus has an immunosuppressive potential [40]. Our data indicated that $m^6A$-defective HIV-1 RNA enhanced RIG-I-mediated RNA sensing and IFN-I induction in cells. Further studies are needed to examine whether the $m^6A$-modified HIV-1 RNA binds RIG-I with a low affinity, which might be the possible cause of reduced IFN-I induction during viral infection.

In summary, our study uncovered a previously unidentified strategy of how HIV-1 RNA escapes the host antiviral innate immune system through $m^6A$ modifications of its RNA genome. HIV-1 RNA $m^6A$ modifications can act as an immune suppressor of RIG-I-mediated viral RNA sensing. Our findings suggest that pharmacological reduction in $m^6A$ modification of HIV-1 RNA may enhance IFN-I-mediated innate antiviral immune responses, thereby inhibiting viral replication.

## Materials and Methods

**Cell culture.** HEK293T cell line was a kind gift from Vineet KewalRamani (National Cancer Institute, USA) and maintained in complete Dulbecco's modified Eagle's medium (DMEM) as described [32]. U937 cell line was obtained from the American Type Culture Collection (ATCC) and maintained in complete RPMI-1640 medium as described [52]. All the cell lines were

maintained at 37 °C in 5% $CO_2$ and tested negative for mycoplasma contamination using a universal mycoplasma detection kit (ATCC 30-1012K) as described [53].

**Plasmids and HIV-1 RNA oligos.** The HIV-1 proviral DNA construct pNL4-3 was used to generate viral stocks as described [19]. For over-expression of the m$^6$A erasers, the corresponding control vectors, pCMV6-FTO, pCMV-ALKBH5 were described [9, 54]. For knockout of eraser genes, CRISPR-Cas9 vectors containing sgControl, sgFTO, and sgALKBH5 were used as described [38]. For RIG-I knockout, pCR-BluntII-Topo-sgRIGI-1 and 2 vectors were described [55], which were kindly provided by Dr. Stacy Horner (Duke University, USA), and the plasmid hCas9 (catalog no. 41815, Addgene) was described [56]. For MDA5 and RIG-I knockdown, shControl, shMDA5 and shRIG-I plasmids [29] were kindly provided by Dr. Yamina Bennasser (Université de Montpellier, France). Four RNA oligo sequences are from the 5′ UTR of HIV-1 genomic RNA (NL4-3 strain) with or without a single m$^6$A site [32], which were commercially synthesized (Integrated DNA Technologies). The sequences and the location of the m$^6$A sites in the conserved GG**A**CU motifs of the HIV-1 genome were described [32] and are listed below: RNA oligo 1 (nt. 235-281, the m$^6$A-modified adenosine is nt. 241):

5′-CGCAGG**A**CUCGGCUUGCUGGAGACGGCAAGAGGCGAGGGGCG-3′.

To eliminate RNA dimerization in our previous RNA binding assays [32], the original dimer initiation sequence of HIV-1 (AAGCGCGC) in oligo 1 was replaced with the underlined nucleotides GAG. RNA oligo 2 (nt. 176-217, the m$^6$A-modified adenosine is nt. 197):

5′-AGCAGUGGCGCCCGAACAGGG**A**CUUGAAAGCGAAAGUAAAGC-3′.

**Generation of U937 cells with MDA5 knockdown or RIG-I knockout, and HEK293T cells with FTO or ALKBH5 knockout.** For MDA5 knockdown U937 cell line construction, HEK293T cells were transfected with shControl or shMDA5, together with pMD2.G and psPAX2 plasmids by polyethyleneimine (PEI) [53]. At 48 h post-transfection, lentiviruses were harvested and purified to infect U937 cells for 48 h and then the U937 cells were selected in RPMI-1640 media with 1 μg/mL puromycin. To generate RIG-I knockout cells, pCR-BluntII-Topo-sgRIGI-I or pCR-BluntII-ToposgRIGI-2, along with hCas9, which has neomycin (G148) resistance, were transfected into U937 cells by TransIT mRNA transfection kit (mirus, USA) for 48 h according to the manufacturer's protocol. Then, G418 (1 mg/mL) was added to transfected cells for 8 days to select RIG-I knockout U937 cells, which were confirmed by Western blotting. For Control, FTO, and ALKBH5 knockout HEK293T cell generation, HEK293T cells were transfected with corresponding single guide RNAs (sgRNAs), together with pMD2.G and psPAX2 plasmids. At 48 h post-transfection, lentiviruses were collected to infect fresh HEK293T cells for 48 h. Then, the single clones were selected by 1 μg/mL puromycin in 96 well plates. The KO cells were confirmed by DNA sequencing and for specific protein expression by Western blotting.

**Dot immunoblotting of m$^6$A modification in RNA.** RNA was extracted from purified and concentrated HIV-1 stocks by using TRIzol (Invitrogen) or RNA purification kit (Qiagen). The synthesized RNA oligos were directly used for dot-blot assays as described [30]. Briefly, HIV-1 RNA or RNA oligos (diluted to 100 μL using 1 mM EDTA) were mixed with 60 μL of 20× saline-sodium citrate (SSC) buffer (3 M NaCl, 0.3 M trisodium citrate) and 40 μL of 37% formaldehyde (Invitrogen) and incubated at 65 °C for 30 min. Nitrocellulose membrane (162-

386 0115, Bio-Rad) or nylon membranes (11209299001, Roche) were pre-soaked with 10X SSC for
387 5 min and assembled in dot-blot apparatus (Bio-Rad) with vacuum-on. Equal amounts of RNA
388 were transferred to nitrocellulose or nylon membranes, then membranes were washed twice with
389 200 μL of 10× SSC buffer. Nylon membranes were washed once with TBST buffer (20 mM Tris,
390 0.9% NaCl, and 0.05% Tween 20) for 5 min and stained with methylene blue staining (MB119,
391 Molecular Research Center) for 2-5 sec followed by two or three washes with dd$H_2O$.
392 Nitrocellulose membranes were blocked with 5% milk in TBST buffer and used to detect $m^6A$
393 levels by probing with $m^6A$ specific antibodies (Synaptic Systems; 202 003). Images were taken
394 by Amersham Biosciences Imager 600 (GE Healthcare) and analyzed by ImageJ software
395 (National Institutes of Health). Densitometry quantification of relative RNA $m^6A$ levels was
396 normalized to MB staining as described [30].
397
398 ***In vitro* FTO demethylation of HIV-1 RNA $m^6A$.** Demethylation of HIV-1 RNA $m^6A$ was
399 performed with recombinant FTO treatment of purified HIV-1 RNA. Briefly, 500 ng HIV-1
400 RNA were used for FTO *in vitro* treatment in 100 μL reaction buffer containing 50 mM HEPES
401 buffer (pH7.0), 75 μM $(NH4)_2Fe\ (SO4)_2 \bullet 6H_2O$, 2 mM L-ascorbic acid, 300 μM L-ascorbic acid,
402 200U RNAsin, 5 μg/mL BSA, and 0.2 nmol FTO protein. The reaction was performed at 37 °C
403 for 1 hr and then stopped by adding 5 mM EDTA. Finally, RNA samples were denatured at
404 70 °C for 2 min and quickly put into ice for $m^6A$ detection.
405
406 **HIV-1 production, p24 quantification, U937 cells transfection and HIV-1 infection assays.**
407 HIV-1 stocks were generated by transfection of HEK293T cells with the proviral DNA pNL4-3
408 using PEI as described [53]. Cell culture medium was exchanged at 6-8 h post-transfection with

supernatants and was harvested at 48 h. The cell culture media containing viruses were filtered (0.45 μm) and purified by 25% sucrose using an SW28 rotor (Beckman Coulter) at 141,000*g* for 90 min. The pellet was resuspended with PBS and digested with DNase I (Turbo, Invitrogen) for 30 min at 37 °C. To extract HIV-1 genome RNA, concentrated HIV-1 virions were lysed by Trizol (Invitrogen) and RNA was purified by phenolic-chloroform sedimentation and isopropanol precipitation. For transfection, cells were treated with 100 ng/mL phorbol 12-myristate 13-acetate (PMA) for 24 h and changed with fresh RPMI-1640 media for another 24 h. PMA-differentiated U937 cells were then transfected with TransIT mRNA transfection kits (Mirus) according to the manufacturer protocol. At 16 h post-transfection, cells were harvest for RT-qPCR analysis. For infection assays, HIV-1 p24 levels were quantified by an enzyme-linked immunosorbent assay (ELISA) using anti-p24-coated plates (The AIDS and Cancer Virus Program, NCI-Frederick, MD) as described [30]. PMA-differentiated U937 cells were infected by equal amounts of HIV-1 (250 pg of p24) for 16 h and then cells were collected for Western blotting or RT-qPCR analysis.

**Antibodies and immunoblotting.** The antibodies used in this study were: anti-GAPDH (AHP1628, Bio-Rad), anti-FLAG (F1804, Sigma-Aldrich), anti-METTL3 (15073-1-AP, Proteintech Group), anti-METTL14 (HPA038002, Sigma-Aldrich), anti-FTO (ab124892, Abcam), anti-ALKBH5 (HPA007196, Sigma-Aldrich), anti-MDA5 (D74E4, Cell signaling), anti-RIG-I (D14G6, Cell signaling), anti-HIV-1 Gag (clone #24-2, the NIH AIDS Reagent Program), anti-IRF3 (124399, Abcam), anti-phospho-IRF3 (49475, Cell Signaling), anti-IRF7 (SC-9083, Santa Cruz), anti-phospho-IRF7 (5184, Cell Signaling) and anti-m$^6$A polyclonal rabbit Ab (202003, Synaptic Systems). Cells were harvested and lysed in cell lysis buffer (Cell

Signaling) supplemented with protease inhibitor cocktails (Sigma-Aldrich). Immunoblotting was performed as described [30]. Detection of GAPDH expression was used as a loading control.

**Quantitative RT-PCR.** Real-time quantitative RT-PCR (qRT-PCR) was performed as described [53] to assess the relative levels of *IFN-α* and *IFN-β* mRNA expression in cells induced by HIV-1 RNA transfection or HIV-1 infection. Following primers (IDT) were used:

*IFN-α*, F 5'-GTACTGCAGAATCTCTCCTTTCTCCT-3'

*IFN-α*, R 5'-GTGTCTAGATCTGACAACCTCCCAGG-3'

*IFN-β*, F 5'-AACTTTGACATCCCTGAGGAGATTAAGC-3'

*IFN-β*, R 5'-GACTATGGTCCAGGCACAGTGACTGTAC-3'

*GAPDH*, F 5'-GGAAGGTGAAGGTCGGAGTCAACGG-3'

*GAPDH*, R 5'-CTGTTGTCATACTTCTCATGGTTCAC-3'

**Ethics statement**. The study using human PBMCs from healthy control subjects and HIV-positive individuals has been approved by the Institutional Review Board of the University of Iowa. The study was conducted according to the Declaration of Helsinki guidelines.

**PBMCs from healthy donors and HIV-1 patients.** Healthy control subjects and HIV-positive individuals attending the University of Iowa HIV Clinic who were receiving ART and had HIV-1 viral load levels below the limit of detection (< 20 copies/mL) for over 6 months were invited to participate in these studies, and all provided written informed consent. HIV-1 viral load was determined using the COBAS® AmpliPrep/COBAS® TaqMan HIV-1 test (Roche). PBMCs were purified using BD Vacutainer® CPT™ Mononuclear cell preparation tubes (BD

Biosciences) as recommended by the manufacturer. Cells were stored in 92% fetal calf serum, DMSO in liquid nitrogen until use. PBMCs were obtained with 9 healthy donors, 6 HIV-1 viremic patients, and 16 HIV-1 patients treated with ART (Supplemental Table 1). Both viral RNA and protein were isolated from these PBMCs at the same day using Ambion Paris RNA and protein extraction kit (ThermoFisher Scientific) and stored in -80 °C until use. The RNA was quantitated using the NanoDrop spectrophotometer (ThermoFisher Scientific) and was used for $m^6A$ dot-blot detection (200 ng) and *IFN-α* and *IFN-β* mRNA analyses as described [53]. The protein was quantitated using Pierce BCA reagent (ThermoFisher Scientific) and subjected to Western blot analysis of the $m^6A$ writers and erasers.

**Statistical analyses.** Data were analyzed using either Mann-Whitney's t-test or the one-way analysis of variance (ANOVA) with Prism software and statistical significance was defined as $P < 0.05$. All experiments were repeated at least three times.

**Acknowledgments**

This work was supported in part by National Institutes of Health grants R01AI150343 and R01AI141495 (to L. W.). We thank Alexis Hawkins for technical assistance in detection cellular $m^6A$ levels of PBMCs, and the Wu lab members for helpful discussions and suggestions. We also thank Michael Cahill for outstanding technical support. The authors appreciate generous reagents from Drs. Yamina Bennasser, Stacy Horner, Vineet KewalRamani, Noam Stern-Ginossar, and the NIH AIDS Reagent Program.

**Author contributions**

S.C., S.K., and N.T. performed experiments and contributed to manuscript preparation. J.W. and J.T.S. provided PBMCs from HIV-1 patients and uninfected individuals, and helped data analyses. L.H. and C.H. provided recombinant FTO and the *in vitro* $m^6A$ demethylation protocol. All authors analyzed data and contributed to experiment design. S.C. and S.K. drafted the manuscript. L.W. conceived the study, supervised the work, and revised the manuscript. All authors contributed to manuscript editing and revision.

**Competing interests**: The authors declare no competing interests.

## References

1. Roundtree IA, Evans ME, Pan T, He C. Dynamic RNA Modifications in Gene Expression Regulation. Cell. 2017;169(7):1187-200. Epub 2017/06/18. doi: 10.1016/j.cell.2017.05.045. PubMed PMID: 28622506; PubMed Central PMCID: PMCPMC5657247.
2. Fu Y, Dominissini D, Rechavi G, He C. Gene expression regulation mediated through reversible m(6)A RNA methylation. Nat Rev Genet. 2014;15(5):293-306. doi: 10.1038/nrg3724. PubMed PMID: 24662220.
3. Meyer KD, Jaffrey SR. Rethinking m(6)A Readers, Writers, and Erasers. Annu Rev Cell Dev Biol. 2017;33:319-42. Epub 2017/08/02. doi: 10.1146/annurev-cellbio-100616-060758. PubMed PMID: 28759256; PubMed Central PMCID: PMCPMC5963928.
4. Zhao BS, Roundtree IA, He C. Post-transcriptional gene regulation by mRNA modifications. Nat Rev Mol Cell Biol. 2017;18(1):31-42. doi: 10.1038/nrm.2016.132. PubMed PMID: 27808276; PubMed Central PMCID: PMCPMC5167638.
5. Shi H, Wei J, He C. Where, When, and How: Context-Dependent Functions of RNA Methylation Writers, Readers, and Erasers. Mol Cell. 2019;74(4):640-50. doi: 10.1016/j.molcel.2019.04.025. PubMed PMID: 31100245; PubMed Central PMCID: PMCPMC6527355.
6. Liu J, Yue Y, Han D, Wang X, Fu Y, Zhang L, et al. A METTL3-METTL14 complex mediates mammalian nuclear RNA N6-adenosine methylation. Nat Chem Biol.

2014;10(2):93-5. doi: 10.1038/nchembio.1432. PubMed PMID: 24316715; PubMed Central PMCID: PMC3911877.

7. Ping XL, Sun BF, Wang L, Xiao W, Yang X, Wang WJ, et al. Mammalian WTAP is a regulatory subunit of the RNA N6-methyladenosine methyltransferase. Cell Res. 2014;24(2):177-89. doi: 10.1038/cr.2014.3. PubMed PMID: 24407421; PubMed Central PMCID: PMC3915904.
8. Jia G, Fu Y, Zhao X, Dai Q, Zheng G, Yang Y, et al. N6-methyladenosine in nuclear RNA is a major substrate of the obesity-associated FTO. Nat Chem Biol. 2011;7(12):885-7. doi: 10.1038/nchembio.687. PubMed PMID: 22002720; PubMed Central PMCID: PMC3218240.
9. Zheng G, Dahl JA, Niu Y, Fedorcsak P, Huang CM, Li CJ, et al. ALKBH5 is a mammalian RNA demethylase that impacts RNA metabolism and mouse fertility. Mol Cell. 2013;49(1):18-29. doi: 10.1016/j.molcel.2012.10.015. PubMed PMID: 23177736; PubMed Central PMCID: PMC3646334.
10. Sommer S, Salditt-Georgieff M, Bachenheimer S, Darnell JE, Furuichi Y, Morgan M, et al. The methylation of adenovirus-specific nuclear and cytoplasmic RNA. Nucleic Acids Res. 1976;3(3):749-65. doi: 10.1093/nar/3.3.749. PubMed PMID: 1272797; PubMed Central PMCID: PMC342938.
11. Bondurant M, Hashimoto S, Green M. Methylation pattern of genomic RNA from Moloney murine leukemia virus. J Virol. 1976;19(3):998-1005. PubMed PMID: 972437; PubMed Central PMCID: PMCPMC354940.
12. Thomason AR, Brian DA, Velicer LF, Rottman FM. Methylation of high-molecular-weight subunit RNA of feline leukemia virus. J Virol. 1976;20(1):123-32. PubMed PMID: 185408; PubMed Central PMCID: PMC354973.
13. Beemon K, Keith J. Localization of N6-methyladenosine in the Rous sarcoma virus genome. J Mol Biol. 1977;113(1):165-79. doi: 10.1016/0022-2836(77)90047-x. PubMed PMID: 196091.
14. Moss B, Gershowitz A, Stringer JR, Holland LE, Wagner EK. 5'-Terminal and internal methylated nucleosides in herpes simplex virus type 1 mRNA. J Virol. 1977;23(2):234-9. PubMed PMID: 196108; PubMed Central PMCID: PMC515825.

15. Aloni Y, Dhar R, Khoury G. Methylation of nuclear simian virus 40 RNAs. J Virol. 1979;32(1):52-60. PubMed PMID: 232187; PubMed Central PMCID: PMCPMC353526.
16. Williams GD, Gokhale NS, Horner SM. Regulation of Viral Infection by the RNA Modification N6-Methyladenosine. Annu Rev Virol. 2019;6(1):235-53. doi: 10.1146/annurev-virology-092818-015559. PubMed PMID: 31283446; PubMed Central PMCID: PMCPMC6884077.
17. Lichinchi G, Gao S, Saletore Y, Gonzalez GM, Bansal V, Wang Y, et al. Dynamics of the human and viral m(6)A RNA methylomes during HIV-1 infection of T cells. Nat Microbiol. 2016;1:16011. doi: 10.1038/nmicrobiol.2016.11. PubMed PMID: 27572442; PubMed Central PMCID: PMCPMC6053355.
18. Kennedy EM, Bogerd HP, Kornepati AV, Kang D, Ghoshal D, Marshall JB, et al. Posttranscriptional m(6)A Editing of HIV-1 mRNAs Enhances Viral Gene Expression. Cell Host Microbe. 2016;19(5):675-85. doi: 10.1016/j.chom.2016.04.002. PubMed PMID: 27117054; PubMed Central PMCID: PMC4867121.
19. Tirumuru N, Zhao BS, Lu W, Lu Z, He C, Wu L. N(6)-methyladenosine of HIV-1 RNA regulates viral infection and HIV-1 Gag protein expression. eLife. 2016;5. doi: 10.7554/eLife.15528. PubMed PMID: 27371828; PubMed Central PMCID: PMCPMC4961459.
20. Shulman Z, Stern-Ginossar N. The RNA modification N(6)-methyladenosine as a novel regulator of the immune system. Nat Immunol. 2020;21(5):501-12. doi: 10.1038/s41590-020-0650-4. PubMed PMID: 32284591.
21. Chan YK, Gack MU. Viral evasion of intracellular DNA and RNA sensing. Nat Rev Microbiol. 2016;14(6):360-73. doi: 10.1038/nrmicro.2016.45. PubMed PMID: 27174148; PubMed Central PMCID: PMCPMC5072394.
22. Schlee M, Hartmann G. Discriminating self from non-self in nucleic acid sensing. Nat Rev Immunol. 2016;16(9):566-80. doi: 10.1038/nri.2016.78. PubMed PMID: 27455396; PubMed Central PMCID: PMCPMC7097691.
23. Rehwinkel J, Gack MU. RIG-I-like receptors: their regulation and roles in RNA sensing. Nat Rev Immunol. 2020:1-15. doi: 10.1038/s41577-020-0288-3. PubMed PMID: 32203325; PubMed Central PMCID: PMCPMC7094958.

24. Rasaiyaah J, Tan CP, Fletcher AJ, Price AJ, Blondeau C, Hilditch L, et al. HIV-1 evades innate immune recognition through specific cofactor recruitment. Nature. 2013;503(7476):402-5. doi: 10.1038/nature12769. PubMed PMID: 24196705; PubMed Central PMCID: PMCPMC3928559.
25. Cingoz O, Goff SP. HIV-1 Is a Poor Inducer of Innate Immune Responses. mBio. 2019;10(1). Epub 2019/02/12. doi: 10.1128/mBio.02834-18. PubMed PMID: 30755516; PubMed Central PMCID: PMCPMC6372803.
26. Ranganath N, Sandstrom TS, Fadel S, Cote SC, Angel JB. Type I interferon responses are impaired in latently HIV infected cells. Retrovirology. 2016;13(1):66. doi: 10.1186/s12977-016-0302-9. PubMed PMID: 27613235; PubMed Central PMCID: PMC5017046.
27. He B, Tran JT, Sanchez DJ. Manipulation of Type I Interferon Signaling by HIV and AIDS-Associated Viruses. J Immunol Res. 2019;2019:8685312. doi: 10.1155/2019/8685312. PubMed PMID: 31089479; PubMed Central PMCID: PMCPMC6476103.
28. Wu L. HIV Evades Immune Surveillance by Methylation of Viral RNA. Biochemistry. 2019;58(13):1699-700. doi: 10.1021/acs.biochem.9b00152. PubMed PMID: 30892021; PubMed Central PMCID: PMCPMC6445747.
29. Ringeard M, Marchand V, Decroly E, Motorin Y, Bennasser Y. FTSJ3 is an RNA 2'-O-methyltransferase recruited by HIV to avoid innate immune sensing. Nature. 2019;565(7740):500-4. doi: 10.1038/s41586-018-0841-4. PubMed PMID: 30626973.
30. Tirumuru N, Wu L. HIV-1 envelope proteins up-regulate N (6)-methyladenosine levels of cellular RNA independently of viral replication. J Biol Chem. 2019;294(9):3249-60. doi: 10.1074/jbc.RA118.005608. PubMed PMID: 30617182; PubMed Central PMCID: PMCPMC6398121.
31. Cohn LB, Chomont N, Deeks SG. The Biology of the HIV-1 Latent Reservoir and Implications for Cure Strategies. Cell Host Microbe. 2020;27(4):519-30. doi: 10.1016/j.chom.2020.03.014. PubMed PMID: 32272077; PubMed Central PMCID: PMCPMC7219958.
32. Lu W, Tirumuru N, St Gelais C, Koneru PC, Liu C, Kvaratskhelia M, et al. N(6)-Methyladenosine-binding proteins suppress HIV-1 infectivity and viral production. J Biol Chem. 2018;293(34):12992-3005. doi: 10.1074/jbc.RA118.004215. PubMed PMID: 29976753; PubMed Central PMCID: PMCPMC6109920.

33. Bader JP, Brown NR, Chiang PK, Cantoni GL. 3-Deazaadenosine, an inhibitor of adenosylhomocysteine hydrolase, inhibits reproduction of Rous sarcoma virus and transformation of chick embryo cells. Virology. 1978;89(2):494-505. doi: 10.1016/0042-6822(78)90191-5. PubMed PMID: 213879.
34. Doyle T, Goujon C, Malim MH. HIV-1 and interferons: who's interfering with whom? Nat Rev Microbiol. 2015;13(7):403-13. doi: 10.1038/nrmicro3449. PubMed PMID: 25915633.
35. Hardy GA, Sieg S, Rodriguez B, Anthony D, Asaad R, Jiang W, et al. Interferon-α is the primary plasma type-I IFN in HIV-1 infection and correlates with immune activation and disease markers. PLoS One. 2013;8(2):e56527. Epub 2013/02/20. doi: 10.1371/journal.pone.0056527. PubMed PMID: 23437155; PubMed Central PMCID: PMCPMC3577907.
36. Jurczyszak D, Zhang W, Terry SN, Kehrer T, Bermudez Gonzalez MC, McGregor E, et al. HIV protease cleaves the antiviral m6A reader protein YTHDF3 in the viral particle. PLoS Pathog. 2020;16(2):e1008305. doi: 10.1371/journal.ppat.1008305. PubMed PMID: 32053707; PubMed Central PMCID: PMCPMC7043784.
37. Rubio RM, Depledge DP, Bianco C, Thompson L, Mohr I. RNA m(6) A modification enzymes shape innate responses to DNA by regulating interferon beta. Genes Dev. 2018;32(23-24):1472-84. doi: 10.1101/gad.319475.118. PubMed PMID: 30463905; PubMed Central PMCID: PMCPMC6295168.
38. Winkler R, Gillis E, Lasman L, Safra M, Geula S, Soyris C, et al. m(6)A modification controls the innate immune response to infection by targeting type I interferons. Nat Immunol. 2019;20(2):173-82. doi: 10.1038/s41590-018-0275-z. PubMed PMID: 30559377.
39. Lu M, Zhang Z, Xue M, Zhao BS, Harder O, Li A, et al. N(6)-methyladenosine modification enables viral RNA to escape recognition by RNA sensor RIG-I. Nat Microbiol. 2020;5(4):584-98. doi: 10.1038/s41564-019-0653-9. PubMed PMID: 32015498; PubMed Central PMCID: PMCPMC7137398.
40. Durbin AF, Wang C, Marcotrigiano J, Gehrke L. RNAs Containing Modified Nucleotides Fail To Trigger RIG-I Conformational Changes for Innate Immune Signaling. mBio. 2016;7(5). doi: 10.1128/mBio.00833-16. PubMed PMID: 27651356; PubMed Central PMCID: PMC5030355.

41. Courtney DG, Tsai K, Bogerd HP, Kennedy EM, Law BA, Emery A, et al. Epitranscriptomic Addition of m(5)C to HIV-1 Transcripts Regulates Viral Gene Expression. Cell Host Microbe. 2019;26(2):217-27 e6. doi: 10.1016/j.chom.2019.07.005. PubMed PMID: 31415754; PubMed Central PMCID: PMCPMC6714563.
42. Martinelli E, Cicala C, Van Ryk D, Goode DJ, Macleod K, Arthos J, et al. HIV-1 gp120 inhibits TLR9-mediated activation and IFN-{alpha} secretion in plasmacytoid dendritic cells. Proc Natl Acad Sci U S A. 2007;104(9):3396-401. doi: 10.1073/pnas.0611353104. PubMed PMID: 17360657; PubMed Central PMCID: PMC1805537.
43. Kaushik S, Teque F, Patel M, Fujimura SH, Schmidt B, Levy JA. Plasmacytoid dendritic cell number and responses to Toll-like receptor 7 and 9 agonists vary in HIV Type 1-infected individuals in relation to clinical state. AIDS Res Hum Retroviruses. 2013;29(3):501-10. doi: 10.1089/AID.2012.0200. PubMed PMID: 23131038; PubMed Central PMCID: PMC3581027.
44. Solis M, Nakhaei P, Jalalirad M, Lacoste J, Douville R, Arguello M, et al. RIG-I-mediated antiviral signaling is inhibited in HIV-1 infection by a protease-mediated sequestration of RIG-I. J Virol. 2011;85(3):1224-36. doi: 10.1128/JVI.01635-10. PubMed PMID: 21084468; PubMed Central PMCID: PMC3020501.
45. Yan N, Regalado-Magdos AD, Stiggelbout B, Lee-Kirsch MA, Lieberman J. The cytosolic exonuclease TREX1 inhibits the innate immune response to human immunodeficiency virus type 1. Nat Immunol. 2010;11(11):1005-13. doi: 10.1038/ni.1941. PubMed PMID: 20871604; PubMed Central PMCID: PMC2958248.
46. Sanchez DJ, Miranda D, Jr., Marsden MD, Dizon TM, Bontemps JR, Davila SJ, et al. Disruption of Type I Interferon Induction by HIV Infection of T Cells. PLoS One. 2015;10(9):e0137951. doi: 10.1371/journal.pone.0137951. PubMed PMID: 26375588; PubMed Central PMCID: PMC4574156.
47. Sirois M, Robitaille L, Allary R, Shah M, Woelk CH, Estaquier J, et al. TRAF6 and IRF7 control HIV replication in macrophages. PLoS One. 2011;6(11):e28125. doi: 10.1371/journal.pone.0028125. PubMed PMID: 22140520; PubMed Central PMCID: PMC3225375.
48. Harman AN, Nasr N, Feetham A, Galoyan A, Alshehri AA, Rambukwelle D, et al. HIV Blocks Interferon Induction in Human Dendritic Cells and Macrophages by Dysregulation

of TBK1. J Virol. 2015;89(13):6575-84. doi: 10.1128/JVI.00889-15. PubMed PMID: 25855743; PubMed Central PMCID: PMC4468486.

49. Okumura A, Alce T, Lubyova B, Ezelle H, Strebel K, Pitha PM. HIV-1 accessory proteins VPR and Vif modulate antiviral response by targeting IRF-3 for degradation. Virology. 2008;373(1):85-97. doi: 10.1016/j.virol.2007.10.042. PubMed PMID: 18082865; PubMed Central PMCID: PMC2312338.

50. Sachdeva N, Asthana V, Brewer TH, Garcia D, Asthana D. Impaired restoration of plasmacytoid dendritic cells in HIV-1-infected patients with poor CD4 T cell reconstitution is associated with decrease in capacity to produce IFN-alpha but not proinflammatory cytokines. J Immunol. 2008;181(4):2887-97. doi: 10.4049/jimmunol.181.4.2887. PubMed PMID: 18684980.

51. Doehle BP, Chang K, Rustagi A, McNevin J, McElrath MJ, Gale M, Jr. Vpu mediates depletion of interferon regulatory factor 3 during HIV infection by a lysosome-dependent mechanism. J Virol. 2012;86(16):8367-74. doi: 10.1128/JVI.00423-12. PubMed PMID: 22593165; PubMed Central PMCID: PMC3421752.

52. Antonucci JM, St Gelais C, de Silva S, Yount JS, Tang C, Ji X, et al. SAMHD1-mediated HIV-1 restriction in cells does not involve ribonuclease activity. Nat Med. 2016;22(10):1072-4. doi: 10.1038/nm.4163. PubMed PMID: 27711056; PubMed Central PMCID: PMCPMC5069697.

53. Chen S, Bonifati S, Qin Z, St Gelais C, Kodigepalli KM, Barrett BS, et al. SAMHD1 suppresses innate immune responses to viral infections and inflammatory stimuli by inhibiting the NF-kappaB and interferon pathways. Proc Natl Acad Sci U S A. 2018;115(16):E3798-E807. doi: 10.1073/pnas.1801213115. PubMed PMID: 29610295; PubMed Central PMCID: PMCPMC5910870.

54. Wei J, Liu F, Lu Z, Fei Q, Ai Y, He PC, et al. Differential m(6)A, m(6)Am, and m(1)A Demethylation Mediated by FTO in the Cell Nucleus and Cytoplasm. Mol Cell. 2018;71(6):973-85 e5. doi: 10.1016/j.molcel.2018.08.011. PubMed PMID: 30197295; PubMed Central PMCID: PMCPMC6151148.

55. Vazquez C, Tan CY, Horner SM. Hepatitis C Virus Infection Is Inhibited by a Noncanonical Antiviral Signaling Pathway Targeted by NS3-NS4A. J Virol. 2019;93(23). doi:

10.1128/JVI.00725-19. PubMed PMID: 31534039; PubMed Central PMCID: PMCPMC6854490.

56. Mali P, Yang L, Esvelt KM, Aach J, Guell M, DiCarlo JE, et al. RNA-guided human genome engineering via Cas9. Science. 2013;339(6121):823-6. doi: 10.1126/science.1232033. PubMed PMID: 23287722; PubMed Central PMCID: PMCPMC3712628.

**Figure legends** (8 main figures and 2 supplemental figures)

**Fig. 1. A single m$^6$A modification of HIV-1 RNA oligos inhibits IFN-I induction in differentiated U937 cells.** **(A)** HIV-1 5′ UTR (nt. 235–281) RNA oligo 1 (50 ng) with (m$^6$A) or without (control, Ctrl) m$^6$A modification were subjected to m$^6$A dot-blot analysis. MB, methylene blue staining (an RNA loading control). **(B)** and **(C)** RNA oligo 1 (250 ng) were transfected into PMA-differentiated U937 cells. After 16 h, *IFN-α* and *IFN-β* mRNA levels were measured by RT-qPCR. Data shown are means ± S.D. of three independent experiments. Mann-Whitney t-test was used for statistical analysis. **(D)** HIV-1 5′ UTR (nt. 176–217) RNA oligo 2 (200 ng) with (m$^6$A) or without (Ctrl) m$^6$A modification were subjected to m$^6$A dot-blot analysis. **(E)** and **(F)** RNA oligo 2 (250 ng) were transfected into PMA-differentiated U937 cells. After 16 h, *IFN-α* and *IFN-β* mRNA levels were measured by RT-qPCR. Data shown are means ± S.D. of three independent experiments. Un-paired t-test was used for statistical analysis. ** $P < 0.005$, compared with Ctrl samples.

**Fig. 2. Inhibition of m$^6$A modifications of HIV-1 RNA by FTO increases IFN-I induction.** **(A)** m$^6$A levels of HIV-1 genomic RNA were reduced by treatment with demethylase FTO and 50 ng of RNAs were used to confirm the m$^6$A levels by the dot-blot assay. **(B)** and **(C)** 250 ng of

the above RNAs were transfected in PMA-differentiated U937 cells. After 16 h, *IFN-α* and *IFN-β* mRNA levels were measured by RT-qPCR. The results are shown as means ± S.D. of three independent experiments. Mann-Whitney t-test was used for statistical analysis. *** $P < 0.0005$, compared with control samples. **(D)** HEK293T cells were transfected with vector control (Vec) or an FTO-expressing plasmid (FTO). After 24 h, HIV-1 proviral DNA clone (pNL4-3) was transfected for 48 h. Then, cell lysates were collected, and Western blotting was performed using indicated antibodies. **(E)** the m$^6$A levels in HIV-1 genomic RNA were determined by the dot-blot assay using 100 ng purified viral RNA derived from Vec or FTO-expressing HEK293T cells. (**F**) and **(G)** PMA-differentiated U937 cells were transfected with 500 ng of HIV-1 RNA or 250 ng of poly(I:C) for 16 h and analyzed for *IFN-α* and *IFN-β* mRNA levels by RT-qPCR. The results are shown as means ± S.D. of three independent assays. Un-paired t-test was used for statistical analysis. * $P < 0.05$, ** $P < 0.005$, compared between FTO and Vec samples. **(H)** and **(I)** PMA-differentiated U937 cells were infected by HIV-1 (250 pg of p24) from Vec or FTO-expressing HEK293T cells for 16 h, and *IFN-α* and *IFN-β* mRNA levels were quantified by RT-qPCR. The results are shown as means ± S.D. of three independent assays. Un-paired t-test was used for statistical analysis. * $P < 0.05$, ** $P < 0.005$, Vec samples were normalized with non-infection samples.

**Fig. 3. Inhibition of m$^6$A modifications of HIV-1 RNA by ALKBH5 increases IFN-I induction. (A)** HEK293T cells were transfected with a vector control (Vec) or an ALKBH5-expressing plasmid (ALKBH5). After 24 h, pNL4-3 was transfected into these cells for 48 h. Western blotting of cell lysates was performed using specific antibodies. **(B)** HIV-1 genomic RNA m$^6$A levels were determined by the dot-blot assay using 100 ng viral RNA from Vec or

ALKBH5-expressing HEK293T cells. **(C)** and **(D)** PMA-differentiated U937 cells were transfected with 500 ng of the indicated HIV-1 RNAs. At 16 h post-transfection, cells were collected for the analysis of *IFN-α* and *IFN-β* mRNA levels by RT-qPCR. The results are shown as means ± S.D. of three repeated assays. * $P < 0.05$, **** $P < 0.0001$. **(E)** and **(F)** PMA-differentiated U937 cells were infected with HIV-1 (250 pg of p24) from Vec or ALKBH5-expressing HEK293T cells for 16 h, and *IFN-α* and *IFN-β* mRNA levels were quantified by RT-qPCR. The results are shown as means ± S.D. of three repeated experiments. Vec samples were normalized with non-infection samples. Un-paired t-test was used for statistical analysis. *** $P < 0.0005$, **** $P < 0.0001$. Vec samples were normalized with non-infection samples. Un-paired t-test was used for statistical analysis.

**Fig. 4. Knockout of erasers increases m$^6$A levels in HIV-1 RNA and reduces IFN-I induction. (A)** A single clone-derived control, FTO or ALKBH5 knockout (KO) HEK293T cells were transfected with pNL4-3 HIV proviral DNA. After 48 h, cells were collected for Western blotting analysis. **(B)** HIV-1 from the KO cells were collected and viral genomic RNA m$^6$A level was determined by the dot-blot assay using 200 ng viral RNA. **(C)** and **(D)** HIV-1 RNA (250 ng) from KO cells were transfected into PMA-differentiated U937 cells. After 16 h, cells were collected for the analysis of *IFN-α* and *IFN-β* mRNA levels by RT-qPCR. The results are shown as means ± S.D. of three repeats with similar result. * $P < 0.05$, *** $P < 0.0005$. Un-paired t-test was used for statistical analysis. **(E)** and **(F)** HIV-1 (250 pg of p24) from KO cells were used to infect PMA-differentiated U937 cells for 16 h, and cells were collected for the analysis of *IFN-α* and *IFN-β* mRNA levels by RT-qPCR. The results are shown as means ± S.D. of three repeats with similar result. ** $P < 0.005$. Un-paired t-test was used for statistical analysis.

**Fig. 5. DAA-treatment reduces m$^6$A modifications of HIV-1 RNA and increases IFN-I induction through IRF3 and IRF7 phosphorylation.** HEK293T cells were treated with solvent (Ctrl, PBS) or DAA (50 μM) for 3 h and then transfected with the HIV-1 proviral DNA pNL4-3. HIV-1 in the supernatants was collected after 48 h. **(A)** HIV-1 p24 levels in the supernatants were measured by ELISA. **(B)** RNA (100 ng) from these viruses used for the m$^6$A dot-blot assay. **(C)** and **(D)** HIV-1 RNA (250 ng) from Ctrl and DAA-treated samples were transfected into PMA-differentiated U937 cells. After 16 h, cells were collected for the analysis of *IFN-α* and *IFN-β* mRNA levels by RT-qPCR. The results are shown as means ± S.D. of three independent experiments. *** $P < 0.0005$, **** $P < 0.0001$. Un-paired t-test was used for statistical analysis. **(E)** and **(F)** HIV-1 (250 pg of p24) from HEK293T cells was used to infect PMA-differentiated U937 cells for 16 h. After 16 h, U937 cells were collected for the analysis of *IFN-I* mRNA levels by RT-qPCR. The results are shown as means ± S.D. of three independent experiments. *** $P < 0.0005$, **** $P < 0.0001$, Ctrl samples were normalized with non-infection samples. Un-paired t-test was used for statistical analysis. **(G)** PMA-differentiated U937 cells were infected with HIV-1 (250 pg of p24) derived from DAA-treated or control HEK293T cells for 4 h, and U937 cell lysates (50 μg proteins/sample) were used for the analysis of the indicated proteins by Western blotting. GAPDH is used as a loading control. The p-IRF3 and p-IRF7 indicate phosphorylated IRF3 and IRF7, respectively.

**Fig. 6. RIG-I senses m$^6$A modification of HIV-1 RNA to induce IFN-I expression. (A)** RIG-I expression levels in control (Con) and RIG-I knockout (sgRIG-I) U937 cells were measured by Western blotting. **(B)** Con and RIG-I KO U937 cells were transfected with 250 ng of poly(I:C).

782 At 16 h post-transfection, cells were collected for the analysis of *IFN-α* and *IFN-β* mRNA levels
783 by RT-qPCR. The results are shown as means ± S.D. of three repeats with similar result. ** $P <$
784 0.005, **** $P < 0.0001$. **(C)** and **(D)** PMA-differentiated Con and RIG-I KO U937 cells were
785 transfected with 250 ng of RNA oligo 1 **(C)** or oligo 2 **(D)**. After 16 h, cells were collected for
786 the analysis of *IFN-α* and *IFN-β* mRNA levels by RT-qPCR. The results are shown as means ±
787 S.D. of three repeated experiments. * $P < 0.05$, ** $P < 0.005$, **** $P < 0.0001$. Un-paired t-test
788 was used for statistical analysis. ns, not significant.
789
790 **Fig. 7. MDA5 has no specific role in m$^6$A modification of HIV-1 RNA to induce IFN-I**
791 **expression. (A)** MDA5 expression levels were measured by Western blotting using control
792 (shCon) and stable MDA5 knockdown (shMDA5) U937 cells. **(B)** shCon and shMDA5 U937
793 cells were transfected with poly(I:C). At 16 h post-transfection, cells were collected for the
794 analysis of *IFN-α* and *IFN-β* mRNA levels by RT-qPCR. The results are shown as means ± S.D.
795 of three repeats with similar result. * $P < 0.05$, ** $P < 0.005$. **(C)** and **(D)** PMA-differentiated
796 shCon and shMDA5 U937 cells were transfected with 250 ng of RNA oligo 1 **(C)** or oligo 2 **(D)**.
797 At 16 h post-transfection, cells were collected for the analysis of *IFN-α* and *IFN-β* mRNA levels
798 by RT-qPCR. The results are shown as means ± S.D. of three repeated experiments.
799
800 **Fig. 8. Increased m$^6$A levels in total RNA of PBMCs from HIV-1 viremic patients. (A)** Total
801 cellular RNA was isolated from the PBMCs of uninfected healthy individuals (control), HIV-1
802 infected individuals without ART (viremic), and HIV-1 infected individuals on ART (ART)
803 were subjected to m$^6$A dot-blot analysis (200 ng RNA). The dots were quantified and normalized
804 to the respective methylene blue control. The m$^6$A level of first control sample (C1) was set as 1.

Each symbol within the column represents each individual's data point. **(B)** and **(C)** The isolated RNA from the PBMCs of the above described three groups of patients were subjected to RT-qPCR for measuring *IFN-α* and *IFN-β* mRNA expression. The values were normalized to their respective internal control (*GAPDH*). Each symbol represents the data from each individual. **(D)** Cell lysates of PBMCs of each group were subjected to Western blotting for $m^6A$ writers (METTL3 and METTL14) and erasers (ALKBH5 and FTO). The bands were quantified using Image J software and normalized to GAPDH control before plotting into this graphical representation. n, the number of healthy donors or patients. Five samples (C6-C9 and V6) were not included in the Western blot analysis due to the lack of sufficient cell lysates. * $P < 0.05$, ** $P < 0.005$. The one-way analysis of variance (ANOVA) nonparametric was used for statistical analysis.

816 **Supplemental Fig. S1-S2 legends**

817

818 **Fig. S1. Detection of RNA m$^6$A modification and writer and eraser proteins in PBMCs**
819 **from healthy donors and HIV-1 patients. (A)** Total cellular RNA was isolated from the
820 PBMCs of three groups; uninfected healthy control individuals (C1-C9), HIV-1 infected
821 individuals without ART (V1-V6) and with ART (A1-A16) were subjected to m$^6$A dot-blot
822 analysis (200 ng RNA/sample). Methylene blue (MB) staining serves as a loading control. Here
823 every blot represents one patient with the code as referred in Supplemental Table 1. **(B)** Cell
824 lysates of PBMCs of each group uninfected healthy individuals (C1-C5), HIV-1 infected
825 individuals without ART (V1-V5) and with ART (A1-A16) were subjected to Western blot
826 analysis. Five samples (C6-C9 and V6) were not included in the Western blot analysis due to the
827 lack of sufficient cell lysates. Equal amount of proteins (10 µg) of whole cell lysate was
828 immunoblotted for m$^6$A writers (METTL3 and METTL14) and erasers (ALKBH5 and FTO)
829 using specific antibodies. GAPDH serves as a loading control. For the densitometry quantitation
830 of METTL3 levels, only one band at an approximate molecular weight of 70 kDa was used.

831

832 **Fig. S2. HIV-1 RNA escapes from innate immune surveillance.** In HIV-1 producer cells,
833 writers add and erasers remove internal m$^6$A modifications (blue dots) of viral RNA,
834 respectively. HIV-1 with m$^6$A-modificed RNA avoids innate sensing in infected myeloid cells,
835 thereby escaping immune surveillance. Overexpression (O/E) of erasers or inhibiting m$^6$A
836 addition with DAA in HIV-1 producer cells generates viruses with m$^6$A-defective viral RNA.
837 When HIV-1 with m$^6$A-defective RNA infects macrophage-like cells, the cytoplasmic RNA
838 sensor RIG-I recognizes unmodified HIV-1 RNA and triggers phosphorylation (indicated by the

letter P) of the transcription factors IRF3 and IRF7. Phosphorylation of IRF3/7 leads to IFN-α/β expression and generates antiviral innate immune responses in HIV-1-infected macrophage-like cells. However, it remains to be established whether $m^6A$-defective HIV-1 RNA enhances binding to RIG-I, thereby inducing IRF3/7 activation and IFN-I expression in cells.

843 **Supplemental Table 1. Details of PBMC samples from healthy control donors (C1-C9),**

844 **HIV-1 viremic patients (V1-V6), and HIV-1 patients on ART (A1-A16)**

845

| Sample code | Donor gender | Infection status | HIV-1 viral load (copies/mL) | Therapy regimen |
|---|---|---|---|---|
| C1 | Male (M) | Uninfected | 0 | No therapy |
| C2 | M | Uninfected | 0 | No therapy |
| C3 | M | Uninfected | 0 | No therapy |
| C4 | M | Uninfected | 0 | No therapy |
| C5 | M | Uninfected | 0 | No therapy |
| C6 | M | Uninfected | 0 | No therapy |
| C7 | M | Uninfected | 0 | No therapy |
| C8 | M | Uninfected | 0 | No therapy |
| C9 | M | Uninfected | 0 | No therapy |
| V1 | M | HIV+Viremic | 120,000 | Pre-therapy |
| V2 | M | HIV+Viremic | 34,000 | Pre-therapy |
| V3 | M | HIV+Viremic | 1,318,000 | Pre-therapy |
| V4 | M | HIV+Viremic | 35,000 | Pre-therapy |
| V5 | M | HIV+Viremic | 16,000 | Pre-therapy |
| V6 | M | HIV+Viremic | 22,909 | Pre-therapy |
| A1 | M | HIV+Suppressed | ND (non-detectable) | Abacavir, Lamivudine, Efavirenz |
| A2 | M | HIV+Suppressed | ND | Tenofovir, emtricitabine, dolutegravir |
| A3 | M | HIV+Suppressed | ND | Abacavir, Lamivudine, dolutegravir |
| A4 | M | HIV+Suppressed | ND | Tenofovir, emtricitabine, dolutegravir |
| A5 | M | HIV+Suppressed | ND | Abacavir, Lamivudine, dolutegravir |

| | | | | |
|---|---|---|---|---|
| A6 | M | HIV+Suppressed | ND | Tenofovir, emtricitabine, Efavirenz |
| A7 | M | HIV+Suppressed | ND | Tenofovir, emtricitabine, dolutegravir |
| A8 | M | HIV+Suppressed | ND | Tenofovir, emtricitabine, dolutegravir |
| A9 | M | HIV+Suppressed | ND | Tenofovir, emtricitabine, Efavirenz |
| A10 | M | HIV+Suppressed | ND | Abacavir, Lamivudine, dolutegravir |
| A11 | M | HIV+Suppressed | ND | Abacavir, Lamivudine, dolutegravir |
| A12 | M | HIV+Suppressed | ND | Abacavir, Lamivudine, Efavirenz |
| A13 | M | HIV+Suppressed | ND | Tenofovir, emtricitabine, elvitegravir, cobicistat |
| A14 | M | HIV+Suppressed | ND | Abacavir, Lamivudine, dolutegravir |
| A15 | M | HIV+Suppressed | ND | Abacavir, Lamivudine, dolutegravir |
| A16 | M | HIV+Suppressed | ND | Abacavir, Lamivudine, dolutegravir |

846

**Fig. 1**

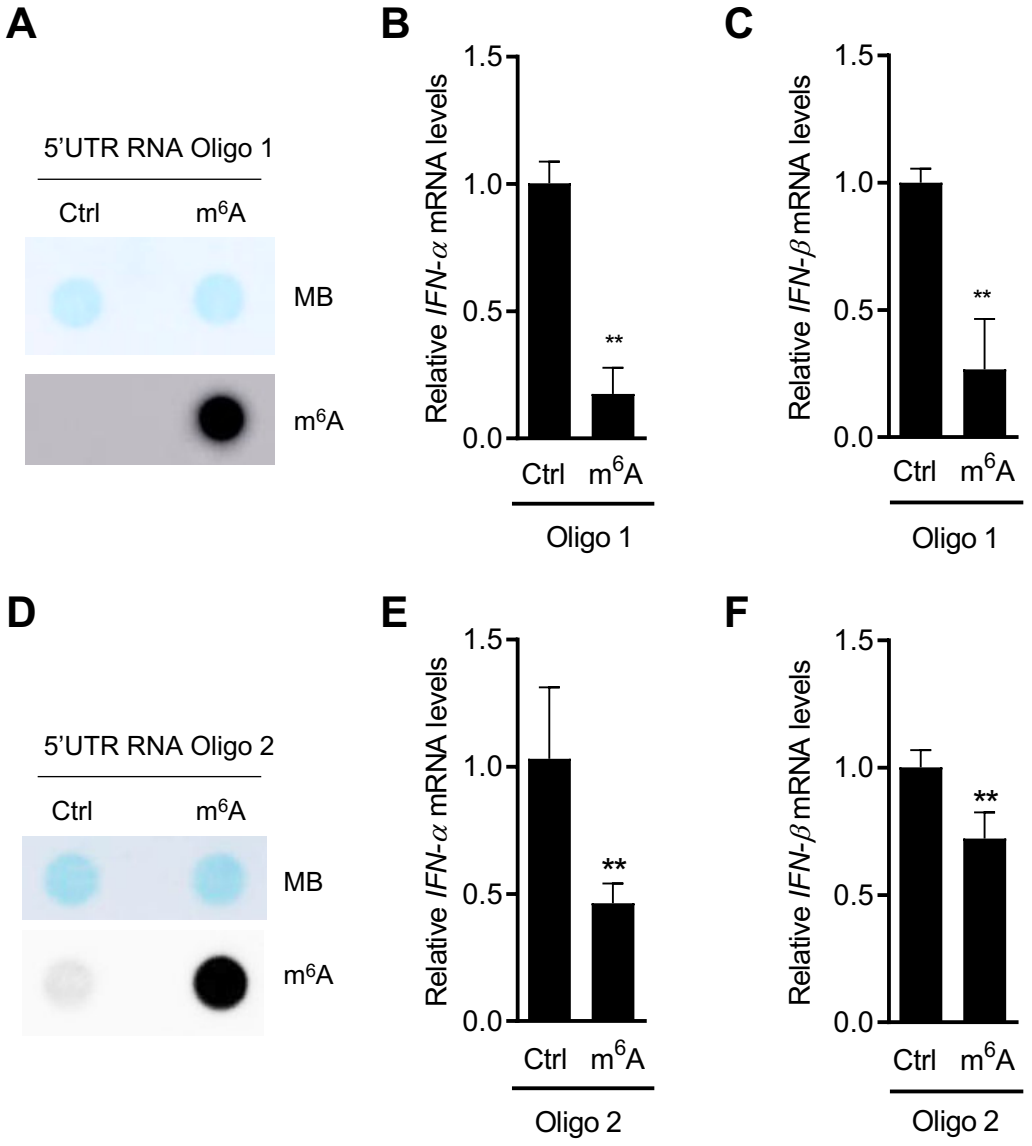
A
5'UTR RNA Oligo 1
Ctrl
m6A
MB
m6A
B
Relative IFN-α mRNA levels
1.5
1.0
0.5
0.0
**
Ctrl
m6A
Oligo 1
C
Relative IFN-β mRNA levels
1.5
1.0
0.5
0.0
**
Ctrl
m6A
Oligo 1
D
5'UTR RNA Oligo 2
Ctrl
m6A
MB
m6A
E
Relative IFN-α mRNA levels
1.5
1.0
0.5
0.0
**
Ctrl
m6A
Oligo 2
F
Relative IFN-β mRNA levels
1.5
1.0
0.5
0.0
**
Ctrl
m6A
Oligo 2

**Fig. 2**

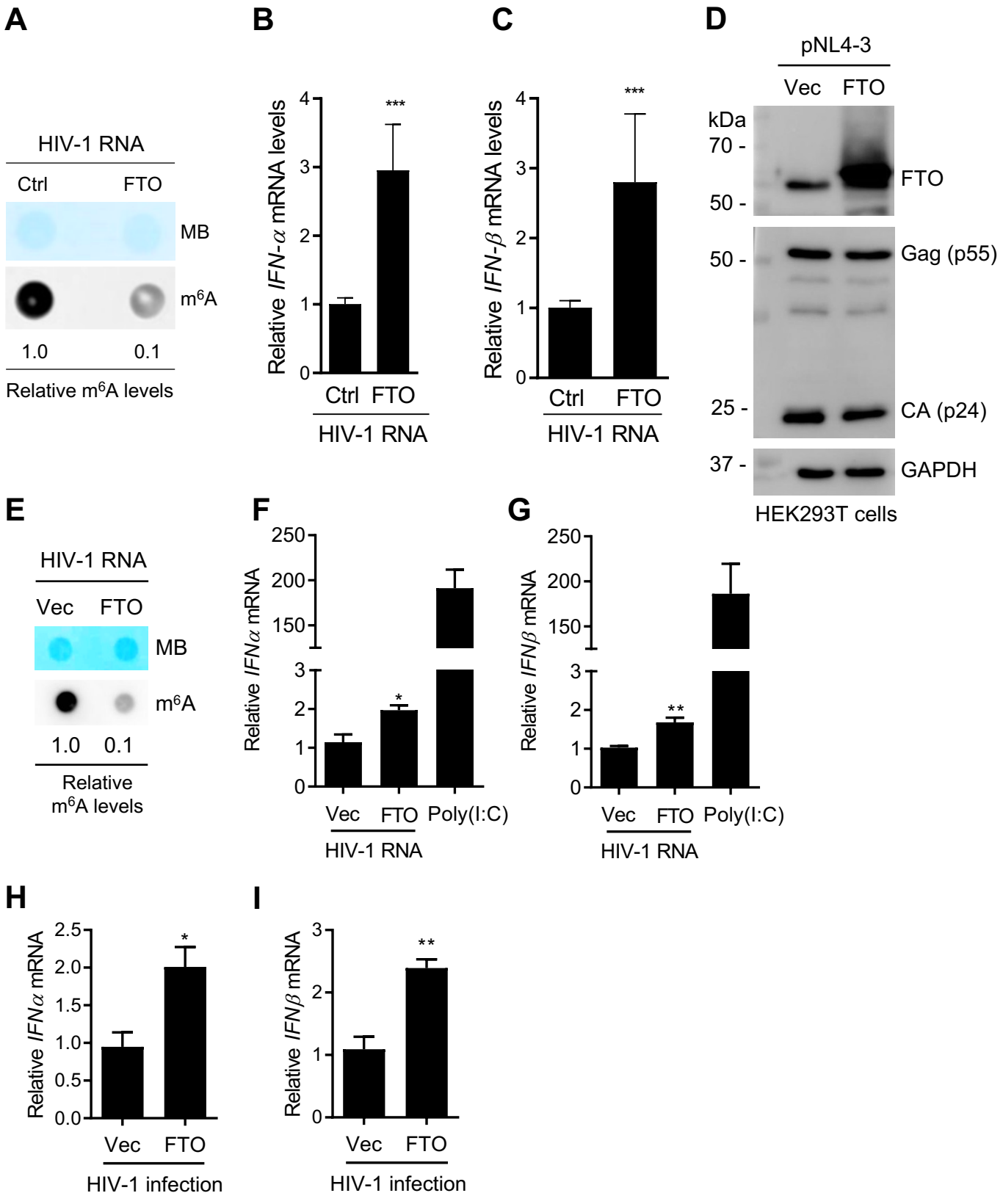
A
HIV-1 RNA
Ctrl
FTO
MB
m6A
1.0
0.1
Relative m6A levels
B
Relative IFN-α mRNA levels
***
Ctrl
FTO
HIV-1 RNA
C
Relative IFN-β mRNA levels
***
Ctrl
FTO
HIV-1 RNA
D
pNL4-3
Vec
FTO
kDa
70 -
50 -
FTO
50 -
Gag (p55)
25 -
CA (p24)
37 -
GAPDH
HEK293T cells
E
HIV-1 RNA
Vec
FTO
MB
m6A
1.0
0.1
Relative m6A levels
F
Relative IFNα mRNA
*
Vec
FTO
Poly(I:C)
HIV-1 RNA
G
Relative IFNβ mRNA
**
Vec
FTO
Poly(I:C)
HIV-1 RNA
H
Relative IFNα mRNA
*
Vec
FTO
HIV-1 infection
I
Relative IFNβ mRNA
**
Vec
FTO
HIV-1 infection

**Fig. 3**

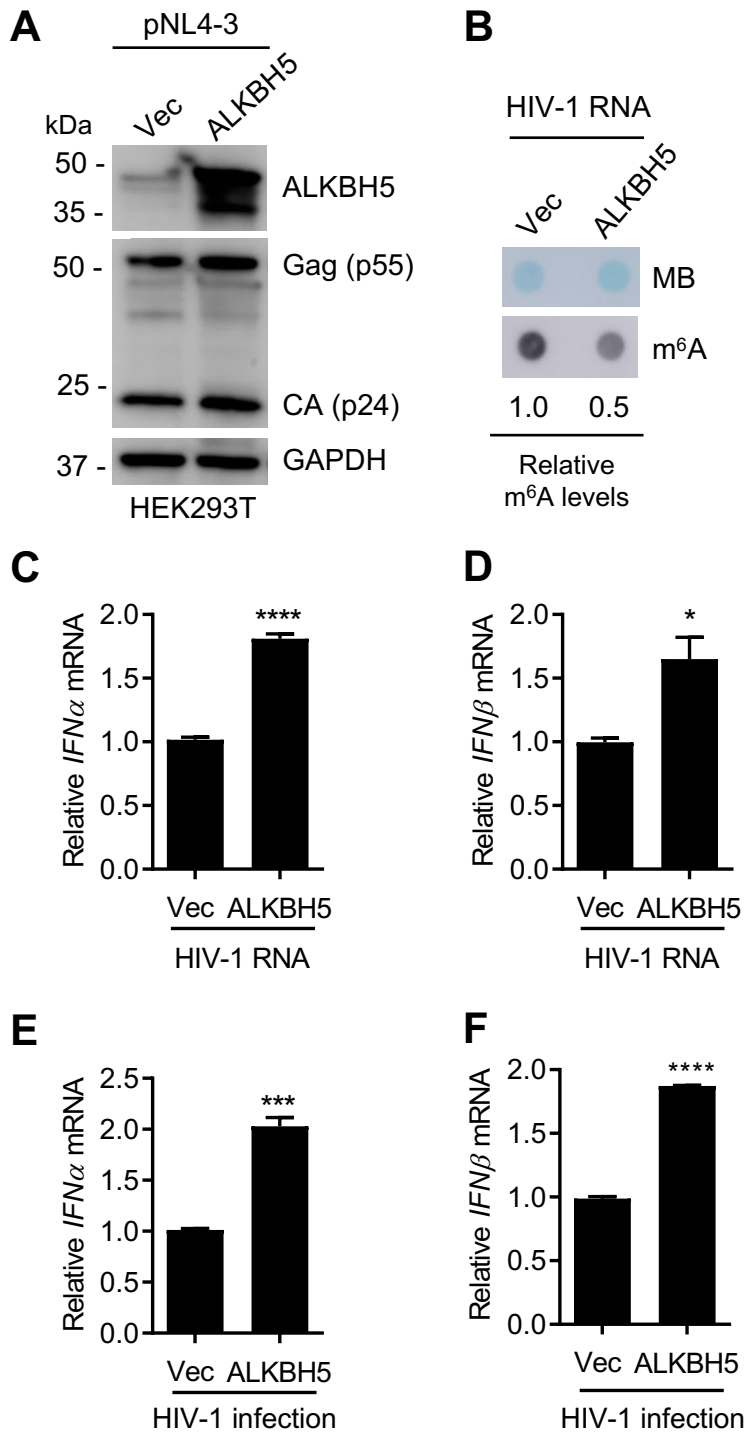
A
pNL4-3
kDa
Vec
ALKBH5
50 -
35 -
ALKBH5
50 -
Gag (p55)
25 -
CA (p24)
37 -
GAPDH
HEK293T
B
HIV-1 RNA
Vec
ALKBH5
MB
m6A
1.0
0.5
Relative m6A levels
C
Relative IFNα mRNA
2.0
1.5
1.0
0.5
0.0
****
Vec
ALKBH5
HIV-1 RNA
D
Relative IFNβ mRNA
2.0
1.5
1.0
0.5
0.0
*
Vec
ALKBH5
HIV-1 RNA
E
Relative IFNα mRNA
2.5
2.0
1.5
1.0
0.5
0.0
***
Vec
ALKBH5
HIV-1 infection
F
Relative IFNβ mRNA
2.0
1.5
1.0
0.5
0.0
****
Vec
ALKBH5
HIV-1 infection

**Fig. 4**

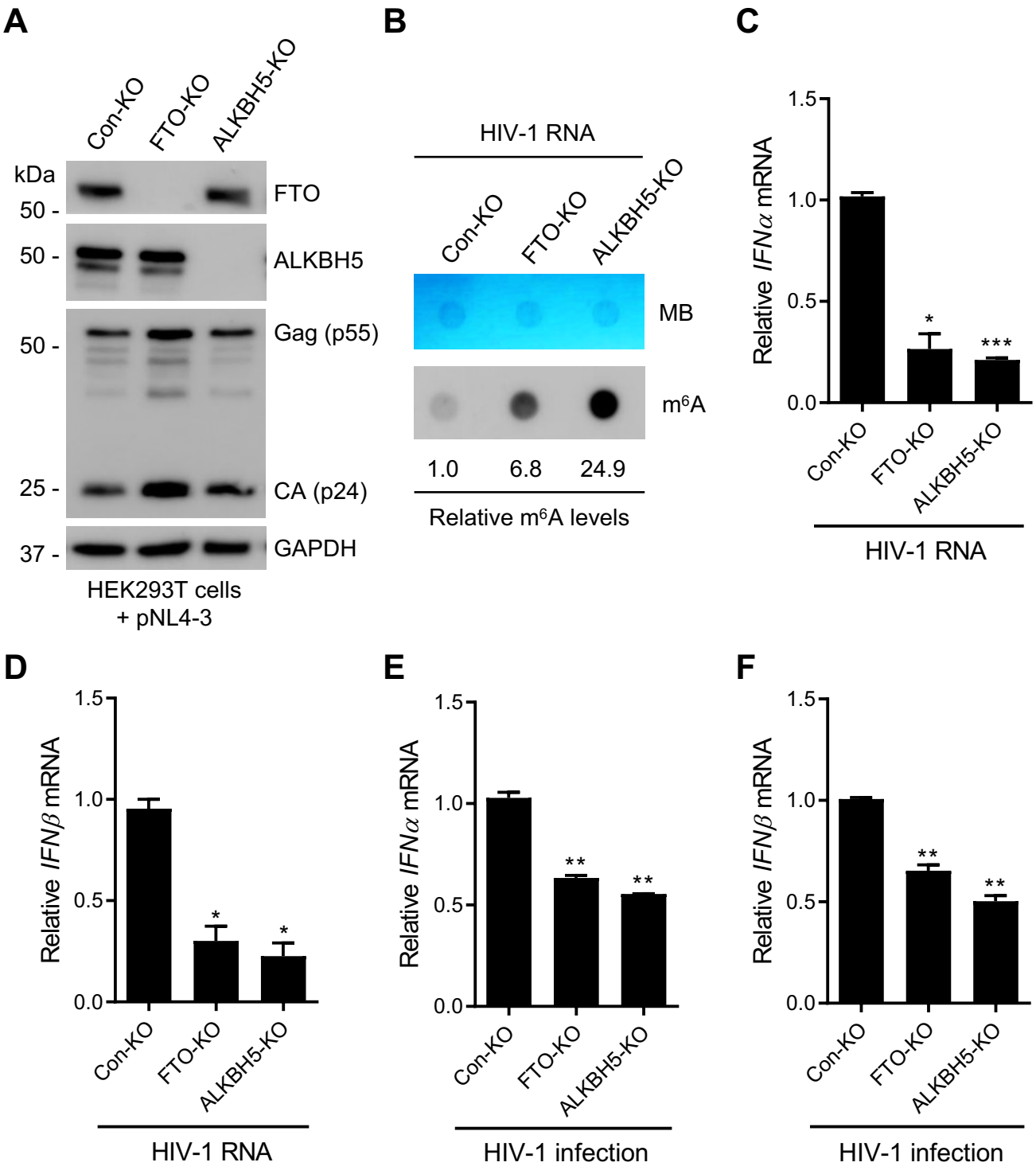
A
Con-KO
FTO-KO
ALKBH5-KO
kDa
50 -
50 -
50 -
25 -
37 -
FTO
ALKBH5
Gag (p55)
CA (p24)
GAPDH
HEK293T cells
+ pNL4-3
B
HIV-1 RNA
Con-KO
FTO-KO
ALKBH5-KO
MB
m6A
1.0
6.8
24.9
Relative m6A levels
C
Relative IFNα mRNA
1.5
1.0
0.5
0.0
*
***
Con-KO
FTO-KO
ALKBH5-KO
HIV-1 RNA
D
Relative IFNβ mRNA
1.5
1.0
0.5
0.0
*
*
Con-KO
FTO-KO
ALKBH5-KO
HIV-1 RNA
E
Relative IFNα mRNA
1.5
1.0
0.5
0.0
**
**
Con-KO
FTO-KO
ALKBH5-KO
HIV-1 infection
F
Relative IFNβ mRNA
1.5
1.0
0.5
0.0
**
**
Con-KO
FTO-KO
ALKBH5-KO
HIV-1 infection

**Fig. 5**

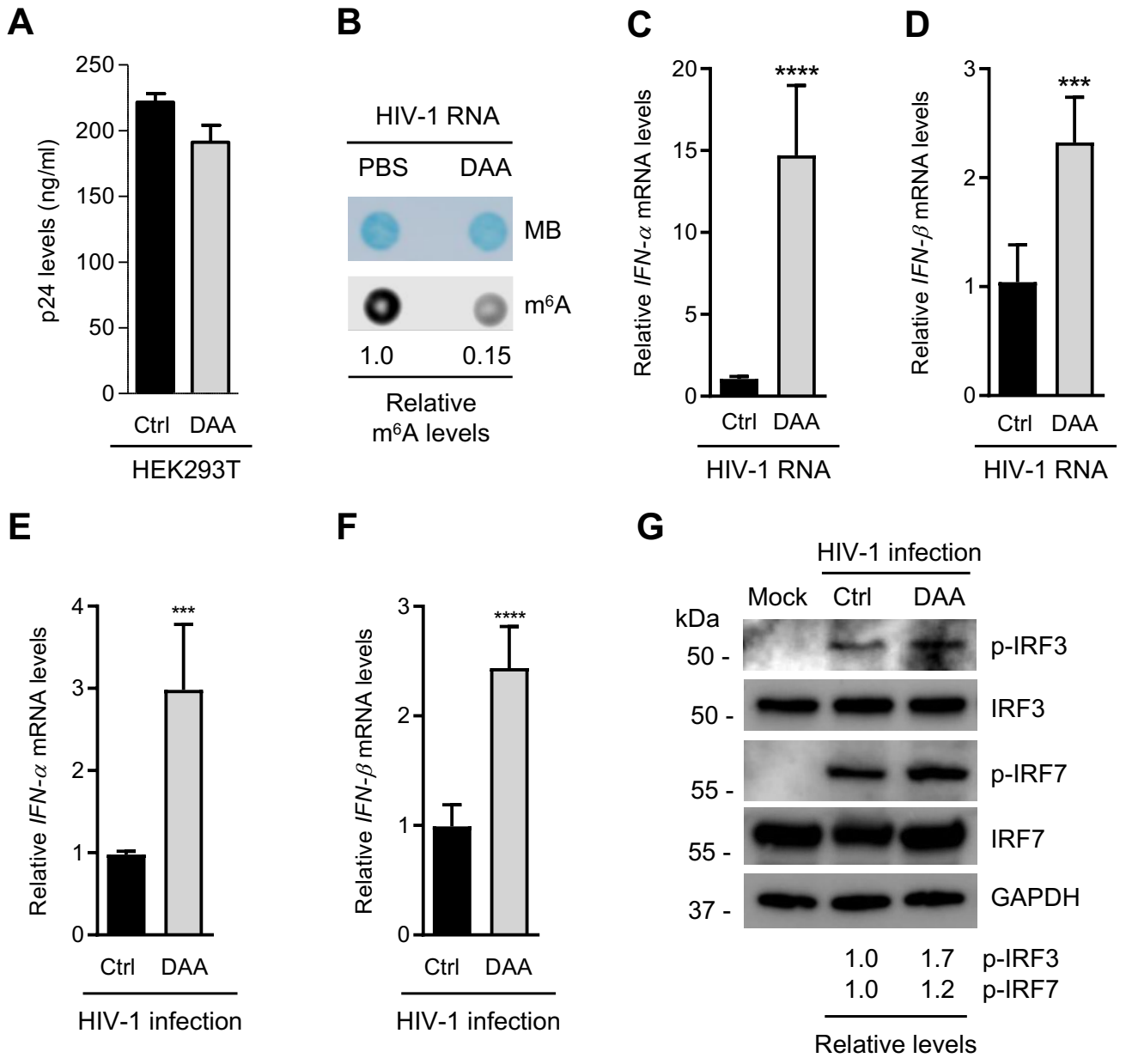
A
p24 levels (ng/ml)
250
200
150
100
50
0
Ctrl
DAA
HEK293T
B
HIV-1 RNA
PBS
DAA
MB
m6A
1.0
0.15
Relative
m6A levels
C
Relative IFN-α mRNA levels
20
15
10
5
0
****
Ctrl
DAA
HIV-1 RNA
D
Relative IFN-β mRNA levels
3
2
1
0
***
Ctrl
DAA
HIV-1 RNA
E
Relative IFN-α mRNA levels
4
3
2
1
0
***
Ctrl
DAA
HIV-1 infection
F
Relative IFN-β mRNA levels
3
2
1
0
****
Ctrl
DAA
HIV-1 infection
G
HIV-1 infection
Mock
Ctrl
DAA
kDa
50 -
p-IRF3
50 -
IRF3
55 -
p-IRF7
55 -
IRF7
37 -
GAPDH
1.0
1.7
p-IRF3
1.0
1.2
p-IRF7
Relative levels

**Fig. 6**

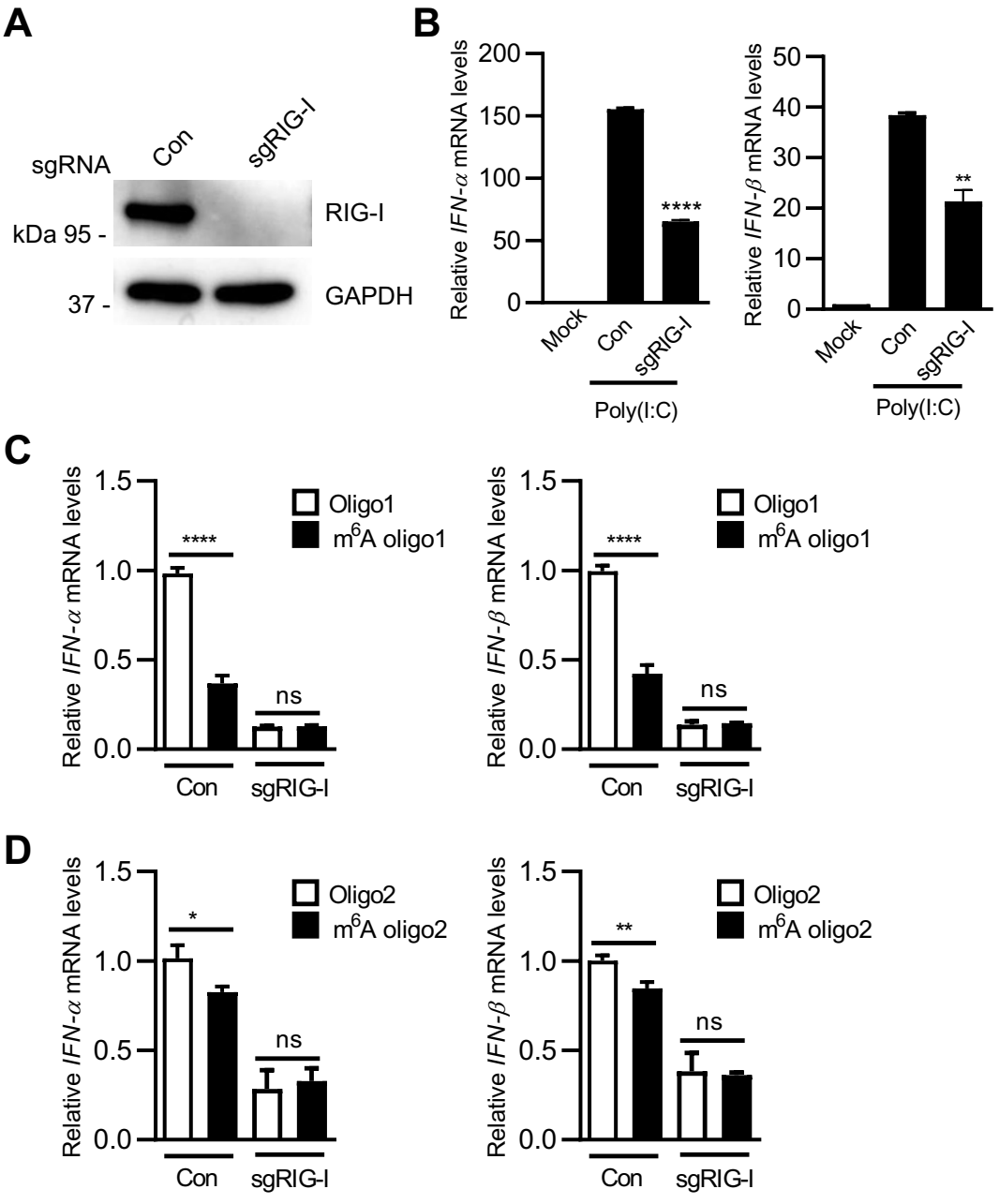
A
sgRNA
Con
sgRIG-I
kDa 95 -
RIG-I
37 -
GAPDH
B
Relative IFN-α mRNA levels
200
150
100
50
0
****
Mock
Con
sgRIG-I
Poly(I:C)
Relative IFN-β mRNA levels
50
40
30
20
10
0
**
Mock
Con
sgRIG-I
Poly(I:C)
C
Relative IFN-α mRNA levels
1.5
1.0
0.5
0.0
****
ns
Oligo1
m6A oligo1
Con
sgRIG-I
Relative IFN-β mRNA levels
1.5
1.0
0.5
0.0
****
ns
Oligo1
m6A oligo1
Con
sgRIG-I
D
Relative IFN-α mRNA levels
1.5
1.0
0.5
0.0
*
ns
Oligo2
m6A oligo2
Con
sgRIG-I
Relative IFN-β mRNA levels
1.5
1.0
0.5
0.0
**
ns
Oligo2
m6A oligo2
Con
sgRIG-I

**Fig. 7**

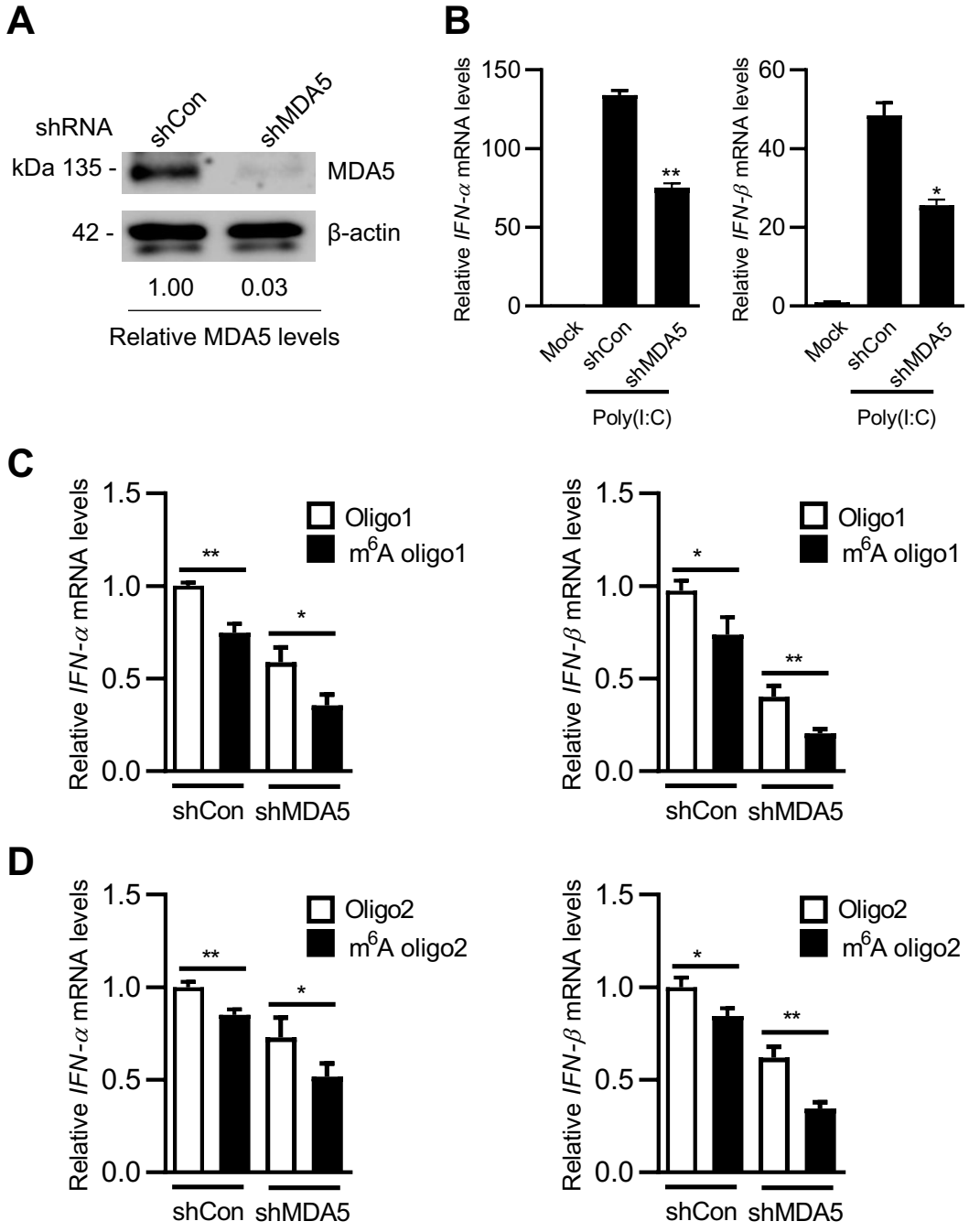
A
shRNA
shCon
shMDA5
kDa 135 -
MDA5
42 -
β-actin
1.00
0.03
Relative MDA5 levels
B
Relative IFN-α mRNA levels
150
100
50
0
**
Mock
shCon
shMDA5
Poly(I:C)
Relative IFN-β mRNA levels
60
40
20
0
*
Mock
shCon
shMDA5
Poly(I:C)
C
Relative IFN-α mRNA levels
1.5
1.0
0.5
0.0
**
*
Oligo1
m6A oligo1
shCon
shMDA5
Relative IFN-β mRNA levels
1.5
1.0
0.5
0.0
*
**
Oligo1
m6A oligo1
shCon
shMDA5
D
Relative IFN-α mRNA levels
1.5
1.0
0.5
0.0
**
*
Oligo2
m6A oligo2
shCon
shMDA5
Relative IFN-β mRNA levels
1.5
1.0
0.5
0.0
*
**
Oligo2
m6A oligo2
shCon
shMDA5

Fig. 8

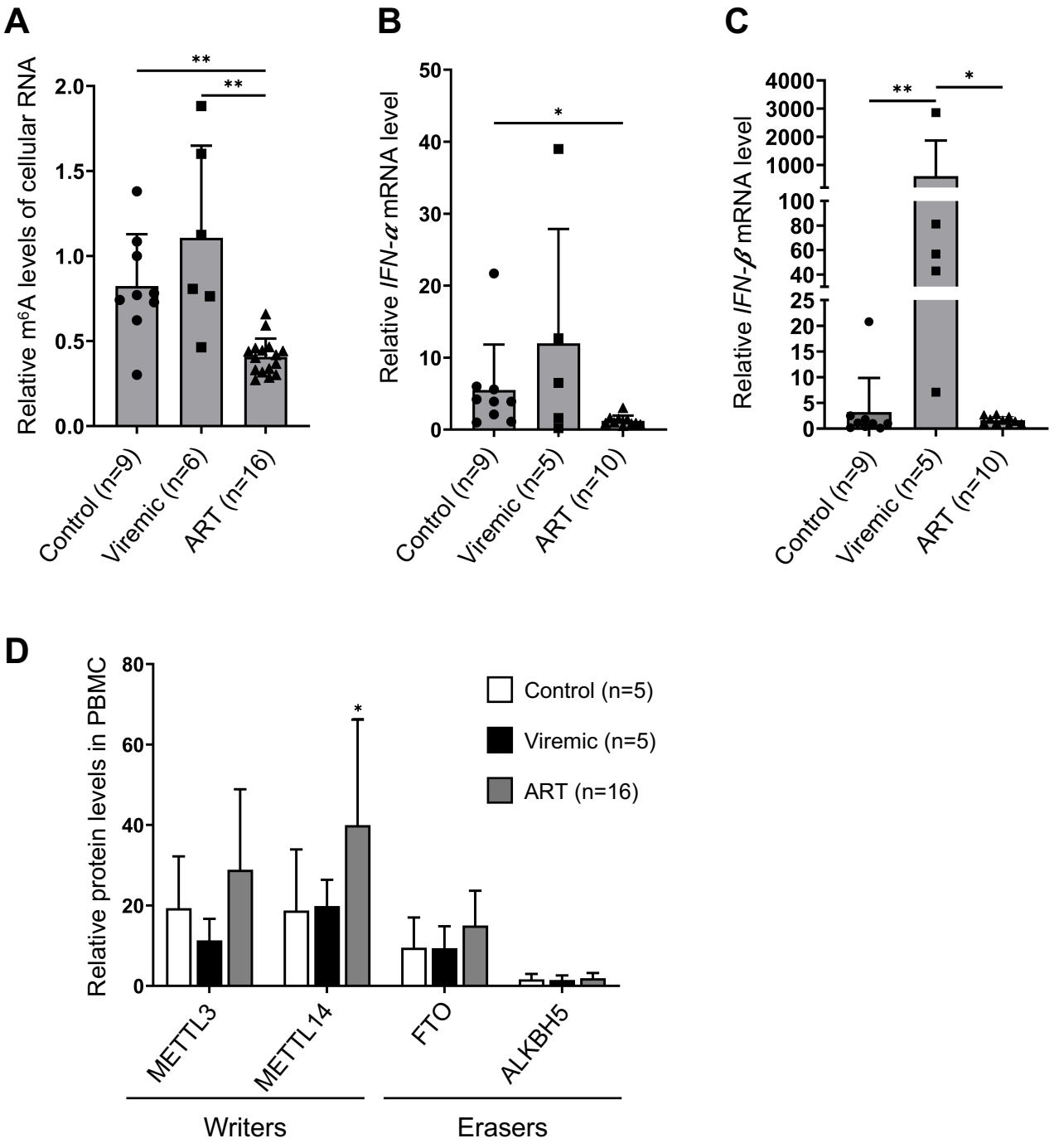
A
Relative m6A levels of cellular RNA
2.0
1.5
1.0
0.5
0.0
**
**
Control (n=9)
Viremic (n=6)
ART (n=16)
B
Relative IFN-α mRNA level
50
40
30
20
10
0
*
Control (n=9)
Viremic (n=5)
ART (n=10)
C
Relative IFN-β mRNA level
4000
3000
2000
1000
100
80
60
40
25
20
15
10
5
0
**
*
Control (n=9)
Viremic (n=5)
ART (n=10)
D
Relative protein levels in PBMC
80
60
40
20
0
*
Control (n=5)
Viremic (n=5)
ART (n=16)
METTL3
METTL14
FTO
ALKBH5
Writers
Erasers

**Supplemental Fig. S1**

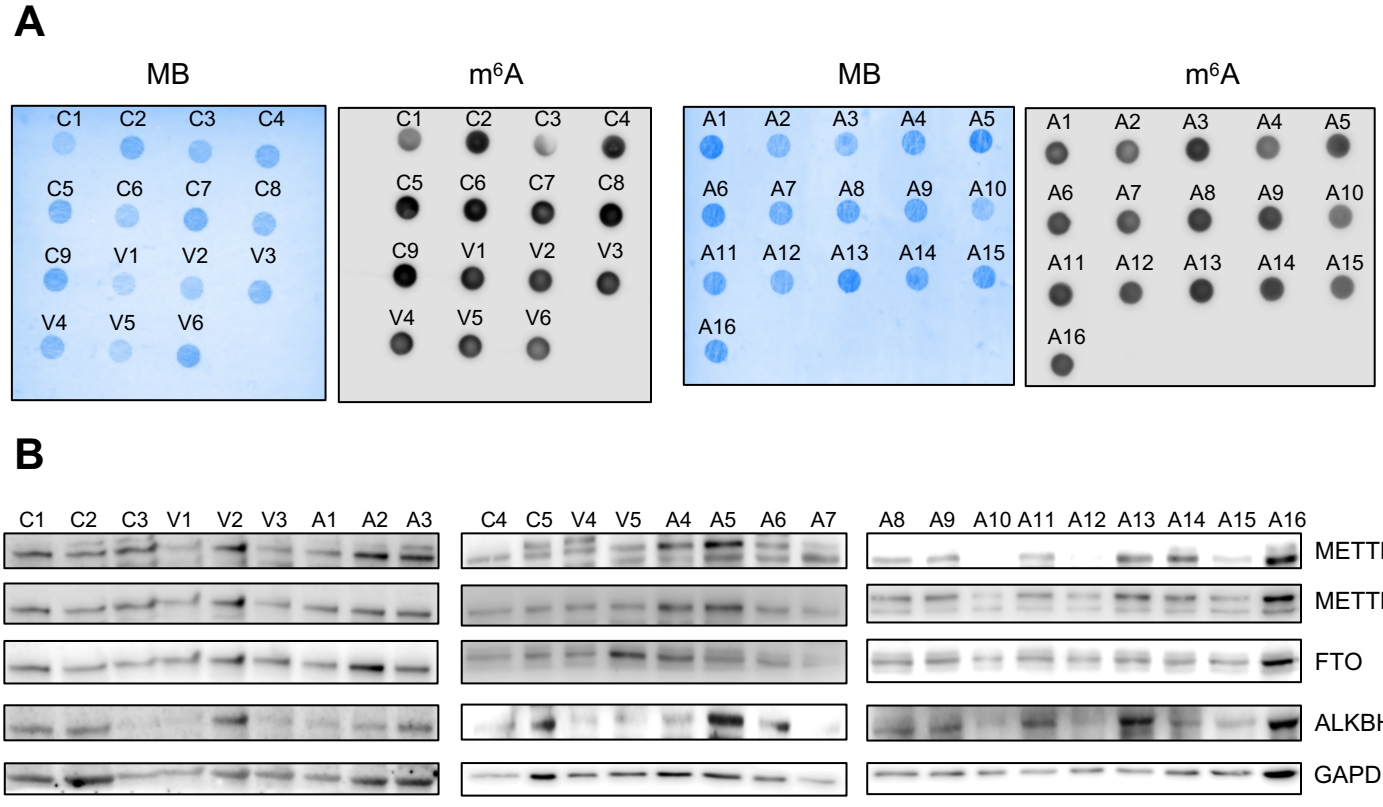

**Supplemental Fig. S2**